Materials Advances

ROYAL SOCIETY OF CHEMISTRY

REVIEW

View Article Online
View Journal | View Issue

Cite this: *Mater. Adv.*, 2022, 3, 6397

Advances of bioactive tellurium nanomaterials in anti-cancer phototherapy

Can Li,[a] Fucheng Gao,[a] Yandong Wang,[a] Li Zhao,[a] Hui Li *[a] and Yanyan Jiang *[ab]

Tellurium nanomaterials show unique advantages, including high carrier mobility, excellent optical properties, and high specific surface areas. Although previous studies have confirmed the application of tellurium nanomaterials in the biological field, their biocompatibility, metabolism, and potential toxicity in organisms demand further exploration. This review systematically summarizes the application of tellurium nanomaterials in the field of tumor phototherapy. Firstly, the common synthesis methods of tellurium nanomaterials are elaborated, mainly including solid-phase deposition, liquid-phase exfoliation, the solution synthesis method, and molecular beam epitaxy. Secondly, the review summarizes the research progress of tellurium nanomaterials in tumor photothermal therapy, photodynamic therapy, photo-triggered molecule delivery, and synergetic therapy. Moreover, we emphasize some breakthroughs in these fields, such as surface-modification and size-control strategies of tellurium nanomaterials. Finally, future prospects are also discussed. The excellent characteristics of tellurium nanomaterials and their relative lack of exploration also suggest that they may have more application opportunities in the near future. This review aims to demonstrate the significance of tellurium nanomaterials in biomedicine and to provide strategies to expand their application in phototherapy.

Received 20th March 2022,
Accepted 29th June 2022

DOI: 10.1039/d2ma00318j

rsc.li/materials-advances

1. Introduction

Cancer, namely malignant tumors, has become a major cause of death because of its uncontrollability and metastasis.[1–3] Currently, the traditional methods of cancer treatment are mainly surgery, radiotherapy, and chemotherapy;[4] however, existing drawbacks such as high risk of recurrence,[5] limited therapeutic effectiveness, damage to normal tissues, and obvious toxicity and side effects[6] demand the development of

[a] *Key Laboratory for Liquid-Solid Structural Evolution & Processing of Materials (Ministry of Education), School of Materials Science and Engineering, Shandong University, Jinan, Shandong, 250061, P. R. China. E-mail: lihuilmy@sdu.edu.cn, yanyan.jiang@sdu.edu.cn*

[b] *Shenzhen Research Institute of Shandong University, Shenzhen, Guangdong, 518057, P. R. China*

Can Li

Can Li is currently pursuing a master's degree within the School of Materials Science and Engineering at Shandong University under the supervision of Professor Yanyan Jiang. She is conducting research on the synthesis of photothermal nanomaterials for antibacterial and anti-cancer applications.

Fucheng Gao

Fucheng Gao is currently a PhD student in the School of Materials Science and Engineering at Shandong University under the supervision of Prof. Yanyan Jiang. He is conducting research on the synthesis of photothermal nanoparticles and clusters for targeting anti-cancer.

new methods of tumor treatment. Due to its unique advantages, including spatiotemporal addressability, minimal invasiveness, relative clinical safety, and high efficiency,[7,8] phototherapy has rapidly developed into a new treatment for malignant tumors and a variety of skin diseases.[9,10]

Nanoparticles belong to a mesoscopic scale, which is located in the transition region between atomic clusters and macro matter. The size of nanomaterials falls within 1–100 nm, which well matches macromolecules in organisms and provides a good crossing ability in tissue gaps. The appropriate size also creates an enhanced permeation and retention (EPR) effect,[7] so some specific macromolecules such as nanoparticles and liposomes[11] are more likely to penetrate and stay in tumor tissues for a long time, which has great advantages for long-term drug release. In addition, the surface of nanomaterials is easy to modify and has the ability to achieve targeted therapy.[12] Therefore, the application of nanomaterials in tumor therapy has always been a research hotspot.

At present, the anticancer nanomaterials that have been clearly confirmed include metal nanoparticles,[13] carbon nanomaterials,[14] two-dimensional (2D) materials[15–17] such as MXenes,[18] inorganic semiconductor nanomaterials,[19] and organic nanoparticles (like micelles or vesicles).[20] The emergence of advanced nanomaterials has also greatly enhanced the development of phototherapies such as photoacoustic imaging,[21] photothermal imaging,[22] fluorescence imaging, and especially photosensitizer-enhanced photodynamic therapy (PDT) and photothermal therapy (PTT).[23] In recent years, some semiconductor materials have been widely explored in the phototherapeutic field because of their excellent physical, chemical, electronic, and optical properties. Among them, as a semiconductor material, tellurium (Te) has attracted a great deal of attention because of several advantages, such as a medium band gap,[24,25] an anisotropic crystal structure, low manufacturing costs, and better environmental stability.[26] Te has great physicochemical reactivity[27] and can generate a rapid response to external stimuli such as a near-infrared (NIR) laser, which is conducive to triggering the release of loaded molecules.[28–30] Especially, the lamellar structure of 2D tellurene (Te nanomaterials with a 2D lamellar structure) provides a high loading capacity for therapeutic molecules and fluorescence

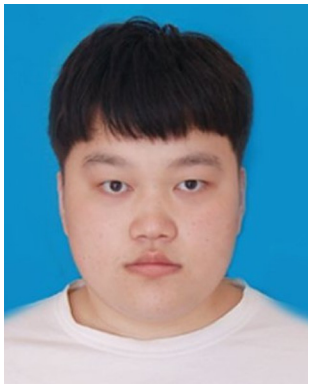

Yandong Wang

Yandong Wang is currently pursuing a master's degree within the School of Materials Science and Engineering at Shandong University under the supervision of Professor Yanyan Jiang. He is conducting research on the synthesis of tumor microenvironment-responsive Fenton sonosensitizers for cancer therapy.

Li Zhao

Li Zhao is currently finishing her PhD in Materials Science and Engineering at Shandong University under the supervision of Prof. Yanyan Jiang. Her current research interests are in the morphological control and functionalization of gold nanoparticles for biological and other applications.

Hui Li

Hui Li received his PhD in 1999 from Shandong University. He then carried out his postdoctoral research in Nanjing University (1999) and University of Trento (2002). He has been promoted to be a full professor since 2005 in the School of Materials Science and Engineering at Shandong University. He has also been appointed as a Taishan Scholar by Shandong Province since 2013. His research interests are in the areas of wetting transformation of novel 2D materials, synthesis of low expansion alloy and refractory alloys and design of nano-electronic devices.

Yanyan Jiang

Yanyan Jiang completed her PhD in Prof. Martina Stenzel group, School of Chemical Engineering at the University of New South Wales, Australia in 2016. She was awarded (2016) Japan Society for Promotion of Science (JSPS) Postdoctoral Research Fellowship at Kyoto University under the supervision of Prof. Itaru Hamachi. Since 2018, she has been appointed as a full professor of materials science and engineering at Shandong University. Her research interests are in the synthesis of functional nanoparticles serving as anticancer drug carriers, biosensors, catalysts, and theoretical studies of the mechanism and properties of these nanoparticles.

factors.[31] Te nanomaterials have various morphologies, such as zero-dimensional nanodots,[32] one-dimensional (1D) nanowires[33,34] or nanotubes, and 2D layered tellurene[35] structures. Moreover, the existence of tellurene has been confirmed by theoretical calculations,[36–38] and its significant light absorption performance has been predicted.[28,31,39,40]

The application of Te in the biomedical field is intriguing. For example, the microbial behavior of Te nanoparticles has been reviewed by Zannoni *et al.*[41] Similarly, others have summarized the synthesis of Te nanomaterials and their application in tumor therapy.[42] Moreover, there are few studies on the metabolism and toxicity mechanism of tellurene materials in organisms,[43] which means there are still many obstacles that need to be overcome. In order to further promote the application of Te nanomaterials in the biomedical field and accelerate their clinical application, this review summarizes the synthetic methods of Te nanomaterials and the mechanism and application of Te nanomaterials in tumor phototherapy, as shown in Fig. 1. In light of the existing problems in application research, this review discusses different perspectives on Te nanomaterials in tumor treatment. Te nanomaterials have great application potential and require further research and exploration.

2. Synthesis of Te nanomaterials

2.1 Structure of Te nanomaterials

Te has many attractive properties, such as photoconductivity, thermoelectricity, and piezoelectricity,[44,45] which makes it an attractive candidate for applications in sensors, optoelectronics, and energy equipment.[46] As a representative element of the *VIA* family, Te is a material with a chain structure and anisotropic characteristics. Te atoms in the chain are connected by strong covalent bonds, as shown in Fig. 2a, while these chains are connected by van der Waals forces, which makes them assume a triangular helix and stack into a hexagonal array,[47] as shown in Fig. 2b. A special chiral chain structure can be observed in tellurene. From Fig. 2c, Te atoms surround an axis parallel to the [0001] direction at the center and corner of the hexagonal basic unit.

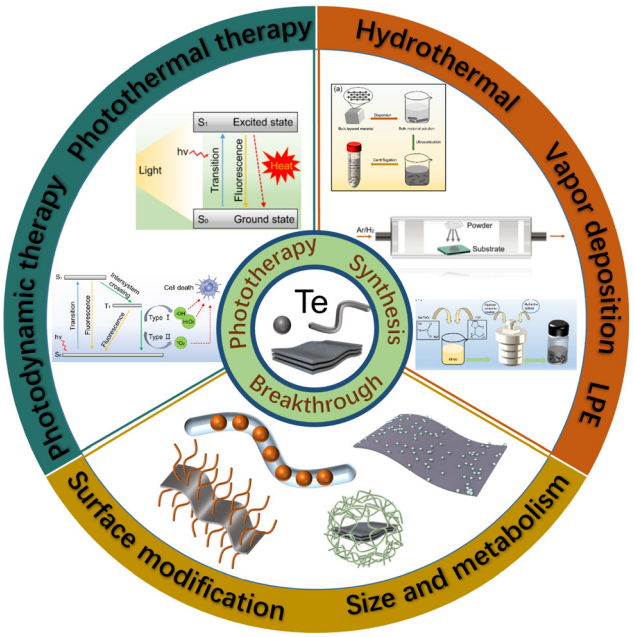

Fig. 1 Summary of synthesis, applications, and breakthroughs of Te nanomaterials.

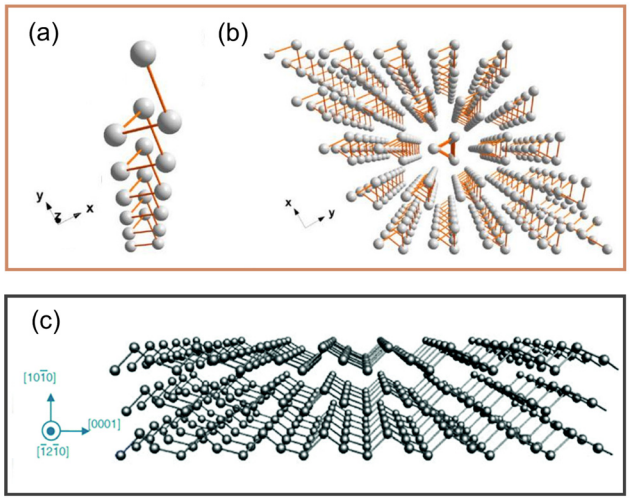

Fig. 2 (a) Structure of single-molecule Te chain.[47] (b) Crystal structure of Te.[47] Copyright 2018, American Chemical Society. (c) Structure of tellurene.[17] Copyright 2019, Royal Society of Chemistry.

For nanomaterials, size and shape are two vital factors that affect their properties.[48,49] Te has a strong tendency to grow as 1D nanostructures because of its chain structure.[27] Therefore, there are numerous synthesis methods to manufacture 1D Te nanoparticles in various forms. However, studies on the synthesis of 2D tellurene nanomaterials are relatively rare. Therefore, exploring the reliable production methods of 2D tellurene materials is of great significance to widen their application in more fields.[50] Taking the above-mentioned points into account, this section highlights the synthesis methods of zero-dimensional and 1D Te nanoparticles and mainly summarizes the synthesis methods of 2D Te nanomaterials.

2.2 Synthesis of zero-dimensional Te nanomaterials

Quantum dots are one of the leaders in the nano field,[51] and they are usually considered zero-dimensional nanomaterials because of their ultra-small size of 1–10 nm;[52–54] we address the synthesis methods of Te nanodots at this scale based on the size of existing quantum dots. Many works have successfully synthesized zero-dimensional Te nanodots with small sizes. Yang *et al.*[55] used $NaBH_4$ to reduce Na_2TeO_3 to produce Te nanodots, which were stabilized with albumin nanocages to yield diameters of 3.4 ± 0.6, 4.6 ± 0.6, and 5.9 ± 0.5 nm by controlling different reaction times, as shown in Fig. 3a–c; they successfully realized size control, which was critical for controlling the properties of the Te nanodots. He *et al.*[56] synthesized Te nanoparticles at room temperature by using oleic acid to oxidize sodium telluride. In this way, an environmentally

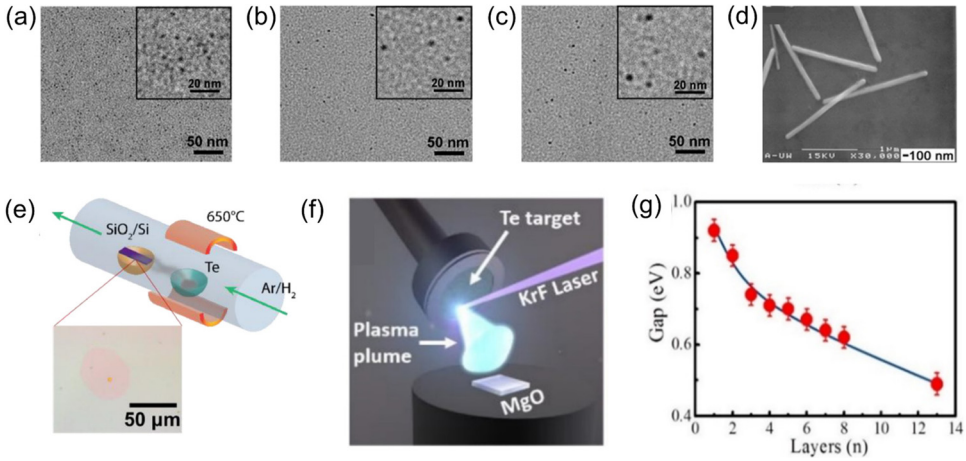

Fig. 3 TEM images of Te nanodots with diameters of (a) 3.4 ± 0.6 nm, (b) 4.6 ± 0.6 nm, and (c) 5.9 ± 0.5 nm.[55] The insets show the corresponding images at a higher magnification. Copyright 2017, American Chemical Society. (d) HR-TEM images of Te nanowires.[34] Copyright 2002, Royal Society of Chemistry. (e) Experimental device diagram of ultrathin Te film prepared by PVD technology.[66] (f) Schematic diagram of the synthesis of tellurene by PLD.[66] Copyright 2019, IOP Publishing. (g) Relationship between the band gap and the thickness of Te films.[75] Copyright 2017, American Chemical Society.

friendly synthetic strategy was developed for Te nanodots with a diameter centered at 1.5 ± 0.5 nm. The obtained Te nanodots could be evenly distributed as thin films *via* electrophoresis, which was also of great significance for the synthesis of 2D nanosheets.

2.3 Synthesis of 1D Te nanomaterials

Considering the chain structure of Te, its 1D form is easy to synthesize. Te can form nanowires with helical atomic chains, and its current density exceeds that of most semiconductor nanowires.[57] Similar to the widely explored carbon nanotubes,[58] except for the third dimension, the other two dimensions remain between 0.1–100 nm, and nanomaterials[58] with a high aspect ratio are considered to have a 1D nanostructure,[59] such as nanowires, nanorods, and nanotubes. The nanowire structure is stable and easy to modify. The hollow structure inside nanotubes endows them with a higher loading efficiency. The synthesis methods of 1D Te nanomaterials have been explored and widely used. At present, many works have realized the synthesis of 1D Te nanostructures, mainly including solid-phase deposition and solution reaction synthesis.

Solid-phase synthesis has been reported in many works. Geng *et al.*[60] prepared 1D Te nanobelts with a length of 50–300 nm and a thickness of 10–20 nm by a simple chemical reaction deposition process of Al_2Te_3 powder and water. In order to realize the controllable growth of 1D Te nanowires, Safdar and colleagues[61] systematically explored the fine structure of Te nanowires, synthesized ordered 1D Te nanostructures by vapor deposition, and proposed more possibilities for their new applications. However, impurities are easy to be mixed in the solid-phase deposition process, and it is still quite difficult to achieve high purity. Thus, solution synthesis provides a better idea.

The cost of solution synthesis is low, and the reaction conditions are relatively not harsh, which ensures the potential of large-scale synthesis. Mayers and Xia[33,34] made a great effort towards the solution synthesis of 1D Te nanomaterials. In their work, Te nanorods with an average length of 1.80 ± 0.16 μm and a width of 98 ± 3 nm were realized (Fig. 3d), and they were able to synthesize nanoneedles, nanotubes, and nanorods with controllable lengths and controllable, uniform interfaces. It is worth noting that telluric acid needed to be decomposed into tellurium dioxide below 150 °C; otherwise, when the temperature was too high, tellurium dioxide would be directly reduced to Te nanorods. Moreover, the obtained samples were not physically degraded after more than one year in the dark. Wen *et al.*[32] synthesized Te nanodot copolymers by the microemulsion method and controlled the photothermal and photodynamic effects by adjusting the ratio of pyrrole to tellurophene to achieve an excellent therapeutic effect. Prangya Bhol *et al.*[62] also prepared Te nanowires as an excellent electrode material by solution reaction. In the work of Kang *et al.*,[63] Te nanorods were grown in an ethylene glycol solvent system, and then some Te was replaced *via* a galvanic reaction to prepare spotted Ru–Te hollow nanorods with better stability, which improved the loading efficiency and realized combined phototherapy. According to the above work, the relatively abundant research on 1D Te nanostructures also lays a good foundation for their subsequent applications.

2.4 Synthesis of 2D tellurene nanomaterials

Research on 2D tellurene nanomaterials is relatively scarce, and their controllable synthesis plays an important role in promoting their application. At present, the existing synthesis methods mainly include physical vapor deposition (PVD),[64–66] liquid-phase exfoliation,[67] and solvothermal synthesis.[35,47]

2.4.1 Physical vapor deposition. PVD technology requires the source material in solid or liquid form to be gasified into gas atoms or molecules under vacuum by physical methods, and then the gaseous material atoms or molecules are controlled to

deposit on the substrate surface to obtain the material film. PVD technology is a common and widely used surface treatment technology[68,69] and can prepare very thin (10^{-7}–10^{-4} m) layers,[70] which plays an extensive and momentous role in the preparation of 2D materials.[71] Several special PVD technologies have emerged, such as vacuum evaporation coating, molecular beam epitaxy (MBE), and pulsed laser deposition (PLD).

Apte *et al.*[66] demonstrated two methods for the growth of ultrathin Te films by PVD. The first one was to use vacuum evaporation coating, where bulk Te was evaporated at 650 °C in an Ar/H_2 atmosphere and then deposited on a Si/SiO_2 substrate and cooled to obtain an ultrathin Te film, which had a typical thickness of 0.85 ± 0.1 nm, as shown in Fig. 3e. The second method utilized PLD technology. Apte *et al.*[66] made use of PLD technology to obtain continuous Te films with a thickness of 2.7–6 nm on a 1 cm × 1 cm single-layer MgO substrate (Fig. 3f). The growth of Te film could be controlled by pulse parameters. In MBE technology,[72] the vapor obtained by heating in an ultrahigh vacuum is directly sprayed onto the substrate, so that the atoms are arranged on the substrate according to the crystal to form a thin film. The use of MBE in the synthesis of tellurene has also been confirmed. Chen *et al.*[45] used MBE to grow Te film on highly oriented pyrolytic graphite.

As a promotion, van der Waals epitaxy (vdWE) combines the substrate and film through weak van der Waals forces, which makes the material fall off more easily and provides a simpler synthesis technology.[73,74] Wang *et al.*[64] used vdWE to grow 2D Te nanosheets on inert mica substrates. After that, Huang *et al.*[75] prepared tellurene on the surface of graphene grown on a 6H–SiC substrate and concluded that the band gap was related to the thickness; that is to say, the band gap decreased monotonically with an increase in Te film thickness, as shown in Fig. 3g. It is worth mentioning that the adjustable band gap (0.49–0.92 eV) covered the mid to NIR spectral range. This was similar to the interaction between MoS_2 and graphene[65] and will lead to the accumulation of local holes, which means that the electronic and optical properties of 2D Te films can be adjusted, a fact that is worthy of our in-depth exploration.

We summarized the above works to show that PVD experiences no chemical reactions in the stacking process and to demonstrate its advantages of less consumption of substrate, uniform and fine film formation, and fast speed.[70,71] Therefore, PVD has strong potential for the preparation of 2D tellurene nanomaterials for biomedical applications, especially uniform and fine Te films expected for tumor treatment.

2.4.2 Liquid-phase exfoliation. Liquid-phase exfoliation (LPE) is a simple technology for preparing 2D nanosheets. Its basic principle is that layered crystals have a strong bonding ability on a 1D plane and a weak bonding between surfaces. Therefore, nanosheets can be stripped from large layered materials by high-speed mixing and stirring (*e.g.*, ultrasonication) (Fig. 4a). At present, graphene,[76] high-quality low-layer antimonene nanosheets,[77] and excellent water-soluble phosphorene[34] have been prepared successively by LPE.

Liu *et al.*[78] obtained large-area 2D tellurene nanosheets in ethanol solvent after ultrasonication and centrifugation. With continuous efforts, Zhang's team[67] prepared 2D layered Te nanostructures with a width of 41.5–177.5 nm and a thickness of 5.1–6.4 nm by LPE. In addition, they also found that 2D Te nanosheets showed excellent optical response under light at wavelengths of 350, 365, 380, and 400 nm, as seen in Fig. 4b and c, which inspires the application of tumor phototherapy in organisms. The use of 2D Te nanosheets prepared by LPE for PDT is reflected in the work of Lin *et al.*,[23] who sonicated raw Te

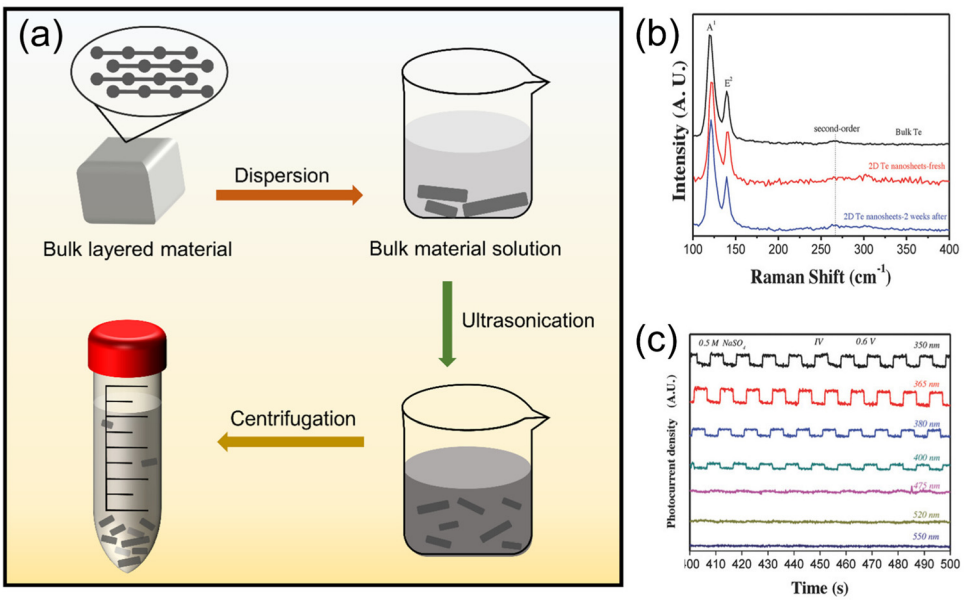

Fig. 4 (a) Schematic of ultrasonic exfoliation to obtain nano-layered materials. (b) and (c) show the photocurrent behavior of 2D Te nanosheets under light at wavelengths of 350, 365, 380, 400, 475, 520, and 550 nm.[67] Copyright 2018, Wiley-VCH.

powder in a dimethylformamide bath to break the bonds of large-size Te layers, and a peeled tellurene nanosheet was obtained.

Compared with the strict requirements of PVD, LPE has the advantages of low cost, simple operation, and low environmental impact,[79] and the latter has the potential to realize mass production. *N*-Methylpyrrolidinone (NMP) has been proven to be one of the successful solvents in LPE technology.[80] Manna *et al.*[79] used a water–NMP mixed solvent system to significantly increase the stripping yield and stabilize the synthesized nanosheets over a long time. Their exploration inspires us to develop a solvent system with good biocompatibility to overcome the obstacles of 2D tellurene applications in the biomedical field, which also opens up a broader scientific perspective for the preparation of nanosheets in more specific biomedical fields. However, controlling the size uniformity of nanomaterials by LPE is still a choke point that limits its application to a certain extent,[81] so further exploration and breakthroughs are needed to solve the existing problems.

2.4.3 Solvothermal synthesis method and other technologies. In addition to PVD and LPE, other technologies have also been explored. Wang and colleagues[35] reported the use of a substrate-free solution process to produce large-area high-quality tellurene. After they stirred Na_2TeO_3 and polyvinylpyrrolidone (PVP) to obtain a uniform solution, they transferred it to a stainless-steel autoclave lined with polytetrafluoroethylene, added ammonia to ensure that the solution was alkaline, and reduced Na_2TeO_3 *via* hydrazine hydrate at a temperature of 160–200 °C to obtain 2D tellurene materials; a schematic diagram is shown in Fig. 5a. The initial product was mainly of a 1D nanostructure; after a period of time, 2D tellurene began to appear, as shown in Fig. 5b. Interestingly, the size and

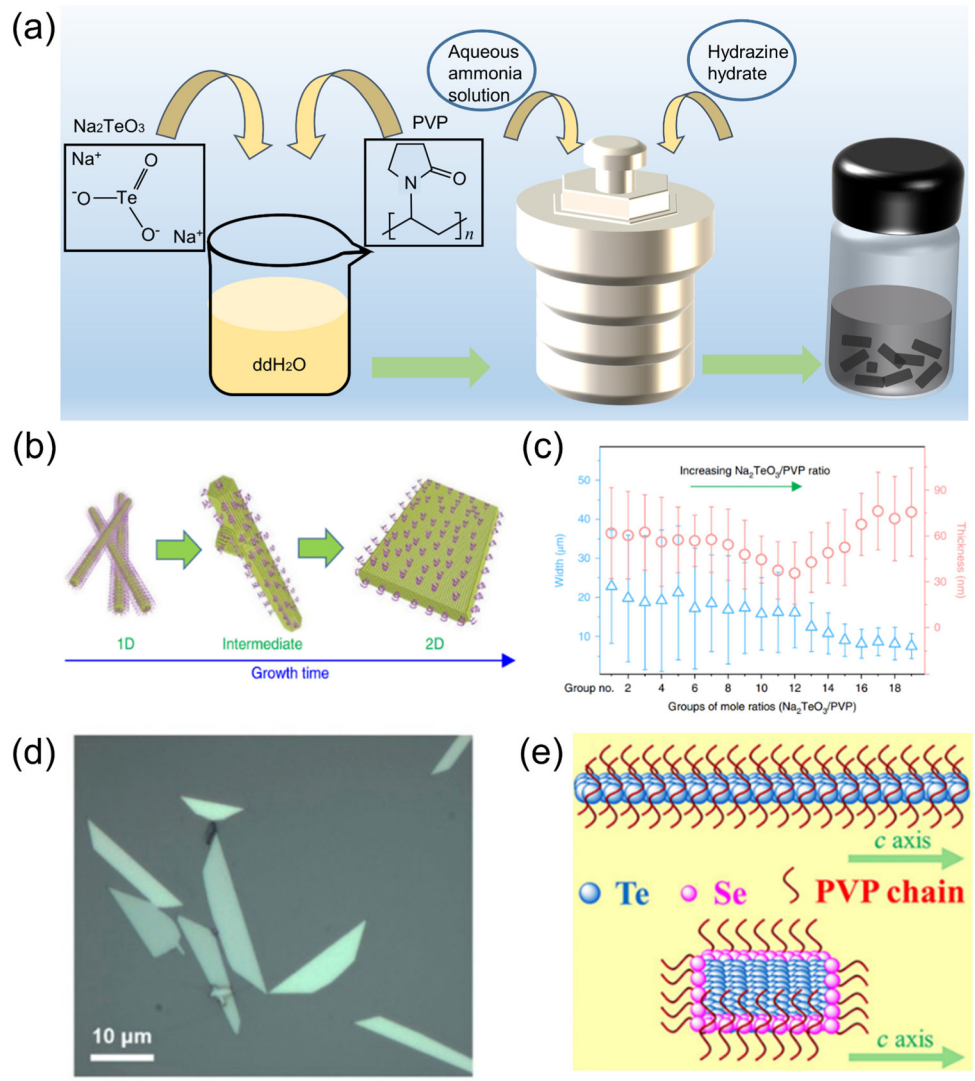

Fig. 5 (a) Schematic diagram of the solvothermal reaction for the synthesis of 2D tellurene. (b) Changes in growth morphology from a 1D Te structure to a 2D Te structure.[35] (c) The growth of 2D tellurene width and thickness for different groups, where each group has a different ratio of Na_2TeO_3/PVP.[35] Copyright 2018, Springer Nature. (d) Optical image of 2D Te nanosheets.[47] Copyright 2018, American Chemical Society. (e) Structure of TeSe nano heterojunction.[83] Copyright 2020, American Association for the Advancement of Science.

thickness of tellurene could be effectively controlled by the ratio of Na_2TeO_3 to PVP, as shown in Fig. 5c. When the ratio of the two was approximately 12 : 1, the average size of tellurene was the smallest, and the width decreased monotonously with a decrease in PVP. This method was also employed in the work of Du *et al.*[82] Amani *et al.*[47] also obtained Te nanosheets through this method, and their thickness was characterized by optical microscopy, as seen in Fig. 5d.

Inspired by the solvothermal synthesis of 2D tellurene, Chen *et al.*[83] prepared selenium-coated Te nano-heterojunctions with a Te phase as the ''core'' and a Se phase as the ''shell.'' The presence of Se causes the Te nanowires to turn into 2D nanosheets (Fig. 5e), with a similar layer structure to tellurene. The solvothermal synthesis method is relatively flexible, and the size and structure of the material can be controlled by the reaction conditions. In addition, some works on the preparation of other 2D nanomaterials provide other possibilities for the synthesis of 2D tellurene, which require further verification. For example, a bismuthene nano-heterojunction was prepared by solvothermal reaction,[84] and antimony was prepared by ultrasonication,[85] which inspired us to think about the preparation of 2D tellurene with a similar structure.

The advantages and disadvantages of these synthesis methods described above are summarized in Table 1. PVD can control the area and thickness of nanosheets through the size of the substrate and the deposition time; the tellurene prepared by this method is of high quality and high purity, and it is likely to be used in fields with precision requirements, but it requires harsh environment. LPE peels large layered materials to yield nanoflakes through ultrasonication or mechanical shear, when the energy of ultrasonic crushing is large, it will be more conducive to the separation of materials. This method is relatively insensitive to the environment, simple, easy to implement, and universal. In the solvothermal strategy, different precursors and the proportion of each component in the reaction are the key factors that control the synthesis size of nanomaterials, it is also possible to synthesize materials with various morphologies and properties, so there are many possibilities for upgrading.

3. Application and breakthrough of Te nanomaterials in tumor phototherapy

Currently, traditional cancer treatment methods such as surgery, radiotherapy, and chemotherapy are still widely used in clinics, which have limited treatment efficacy and serious side effects.[86–88] Therefore, it is necessary to develop a targeted, effective, and efficient treatment method to eliminate cancer cells while causing negligible damage to normal tissues. In recent years, phototherapies such as PTT and PDT have attracted significant attention because of their advantages of fewer traumas, lower toxicity, and better selectivity.[8,89] Phototherapy is a treatment method that gathers photothera peutic reagents at the tumor tissue and irradiates the target area with a light source, especially an NIR light source.

In phototherapy, in addition to the excitation light, the conversion ability of a photosensitizer under radiation is also a pivotal factor for effectiveness, like common inorganic and organic materials[90] such as zinc phthalocyanine, chlorin e6, indocyanine green, graphene quantum dots, gold nanorods,[13] and copper sulfide nanosystems.[91] At present, there are many gaps in Te nanomaterials; for example, the controllable synthesis of 2D tellurene and the potential toxicity of Te nanomaterials. Generally, Te nanomaterials have many applications because of their good electrical conductivity. Especially, the thin layer structure gives 2D tellurene a high specific surface area and high drug loading. Te nanomaterials can also produce heat or cytotoxic reactive oxygen species (ROS) under laser irradiation,[23,92] indicating that they have great potential applications in tumor phototherapy.

3.1 Properties of Te nanomaterials

Te is a p-type semiconductor material[93] with an unusual anisotropic crystal structure and a high melting point of ~450 °C;[64,94] under certain radiation conditions, it will produce active electrons and vacancies, react with the surrounding environment, and cause oxidative stress,[95] which is very similar to the death caused by intracellular ROS during PDT. At the same time, 2D tellurene has great advantages in loading other substances in the application of active catalysis and drug-loaded therapy. The traditional drug delivery platform based

Table 1 Advantages and disadvantages of current technologies for the production of 2D tellurene

	Advantage	Disadvantage
PVD	• Thin, uniform and continuous films • High accuracy • Fast speed • Strong condition controllability	• Harsh environment usually under ultra-high vacuum • The size and thickness of the film can be adjusted by changing the deposition conditions
LPE	• Simple operation and easy implementation • Low cost • Insensitive to environmental conditions • Suitable for mass production	• Difficult to control the size uniformity of materials • Difficult to separate
Solvothermal	• High stability • High flexibility	• Slow method

on nanoparticles usually only has a 10–30% (w/w%) drug loading capacity,[96] while the high surface area of tellurene will produce strong surface interactions with therapeutic or diagnostic molecules, and the loading rate of chemotherapy drugs even reaches 162%.[97] Therefore, Te materials have great potential in PDT[98] and broad application prospects in the biomedical field.

3.2 Application and mechanism of Te nanomaterials in tumor phototherapy

Te-nanomaterial-mediated anticancer phototherapy mainly refers to PTT, PDT, photo-triggered molecule delivery, and their synergetic strategies. Compared with ultraviolet-visible (UV-Vis) light, NIR light used in phototherapy has a larger penetration depth and is a better choice for superficial and deep malignant tissues.[89]

3.2.1 PTT application. The basic principle of PTT is that the heat-resistant temperature of cancer cells is lower than that of normal cells. When the local temperature reaches approximately 42 °C, cancer cells will die due to factors such as protein denaturation, weakening of DNA synthesis and repair.[99] Photothermal materials target and identify cancer cells and gather at the tumor site; they then convert light into heat[100] and reach temperatures above 50 or even 60 °C under NIR irradiation, so as to kill cancer cells. The premise of efficient PTT is to develop a photothermal agent with high photothermal conversion efficiency and good biocompatibility.[90]

As a thickness-dependent bandgap (0.35–1.2 eV) semiconductor nanomaterial,[101,102] Te will generate and relax electron–hole pairs[103] as a narrow bandgap semiconductors such as CuS and MoS_2,[104,105] as shown in Fig. 6a. Therefore, Te nanomaterials can generate a rapid response to NIR lasers,[28–30] which helps to achieve deeper tissue penetration. Wu *et al.*[37] explored the strong light absorption (Fig. 6b) of a few layers of Te. In addition, similar to Mxenes, the layered structure of tellurene causes light waves to reflect between layers and greatly improves the absorption of light energy.[106] Studies have shown that the photothermal conversion efficiency (η) of Te nanosheets is calculated to be 55% under an 808 nm laser,[97] which is significantly higher than bismuthene (19.4%)[107] and traditional graphene oxide (22%)[108] at the same wavelength. These studies have confirmed that Te nanomaterials have a good light absorption effect and high photothermal conversion performance under NIR, which is undoubtedly very attractive in the application of PTT.[28,109,110]

The mushroom polysaccharide–protein complex modified Te nanorods prepared by Huang *et al.*[111] realized high stability in the physiological environment, high selectivity to tumor cells, and efficient tumor ablation. In addition, a high-yield synthesis was achieved by a simple redox method, which was a great impetus to the subsequent development of multifunctional nanosystems. Duan *et al.*[112] developed a functionalized Te nanosystem (DOX/PEI@TeNPs) with good photothermal effectiveness in the NIR region, as shown in Fig. 6c. The DOX/PEI@TeNPs arrived directly at the tumor tissue, and then the anticancer drug doxorubicin hydrochloride (DOX) was released under light control (Fig. 6d), which greatly reduced the damage to normal tissue. This study provided an effective strategy for the design of nanodrug systems and realized precise chemotherapy/PTT synergistic tumor treatment.

Some studies have also explored 2D tellurene. Zhang's team prepared a TeSe nano-heterojunction similar to tellurene,[83] finding it to produce an extremely high photothermal effect and provide efficient cancer treatment. Then, Pan *et al.*[97] prepared and characterized tellurene; modifying with polyethylene glycol (PEG), they obtained Te–PEG-NSs with an average size of approximately 90 nm by using LPE and realizing the application of PTT/chemotherapy, as shown in Fig. 6e. Under the irradiation of an 808 nm laser, the Te–PEG-NSs showed good photothermal stability (Fig. 6f) and achieved a conversion efficiency of 55%, which was significantly higher than some other forms of Te nanomaterials. The significant death of 4T1 cells shown in Fig. 6g and the obvious inhibition of tumor volume both validated the synergistic therapeutic effect of PTT and chemotherapy, which confirmed the superiority of Te nanomaterials as phototherapeutic agents.

The relatively simple synthesis method and adjustable size of Te nanomaterials are very important for the design of nano drug-delivery platforms. Zhang's team found that Te nanoneedles could induce mitochondrial dysfunction and enhance the antioxidant activity of scavenging free radicals with an NIR laser,[113] which provided a new breakthrough for Te nanomaterials in the field of cancer phototherapy.

3.2.2 PDT application. PDT uses photosensitive chemicals (photosensitizers), which can react with molecular oxygen in cells to produce ROS such as singlet oxygen to kill tumor cells. ROS destroy cell membranes, protein structure, and DNA through oxidative stress to damage cancer cells.[89,114] The photodynamic reactions involved in PDT can generally be divided into type I and type II (Fig. 7a).[115] In type I reactions, excited photosensitizers interact with the cell membrane or biological macromolecules to generate free radicals and interact with oxygen to generate substances such as hydrogen peroxide to oxidize the liposome,[116] eventually leading to the rupture of the cell membrane. Type II refers to exciting photosensitizers that transfer energy to oxygen molecules to produce singlet oxygen ($^1O_2$) with strong cytotoxicity. However, the lifetime of 40 ns and the maximum action radius of 20 nm[116] of $^1O_2$ determine that the location of the photosensitizer is the area where PDT can produce direct tissue damage. PDT has been clinically approved for a variety of diseases,[117] such as atherosclerosis and psoriasis. Since the generation of ROS requires huge energy, wavelengths in the range of 650–850 nm are generally considered suitable for PDT.[118] Studies have shown that a few layers of Te can have strong light absorption from UV to visible light, which provides an excellent prerequisite for their application in PDT.[37]

Xu *et al.*[120] realized the PDT of organic phosphorescent materials by exploring the bonding between π-conjugated scaffolds and chalcogenide elements, providing a new platform for the next generation of efficient photosensitizers. In terms of Te nanomaterials, Te nanorods synthesized by Kang *et al.*[63] showed excellent nano enzyme activity, "catalyzed the production of oxygen from hydrogen dioxide, and alleviated the

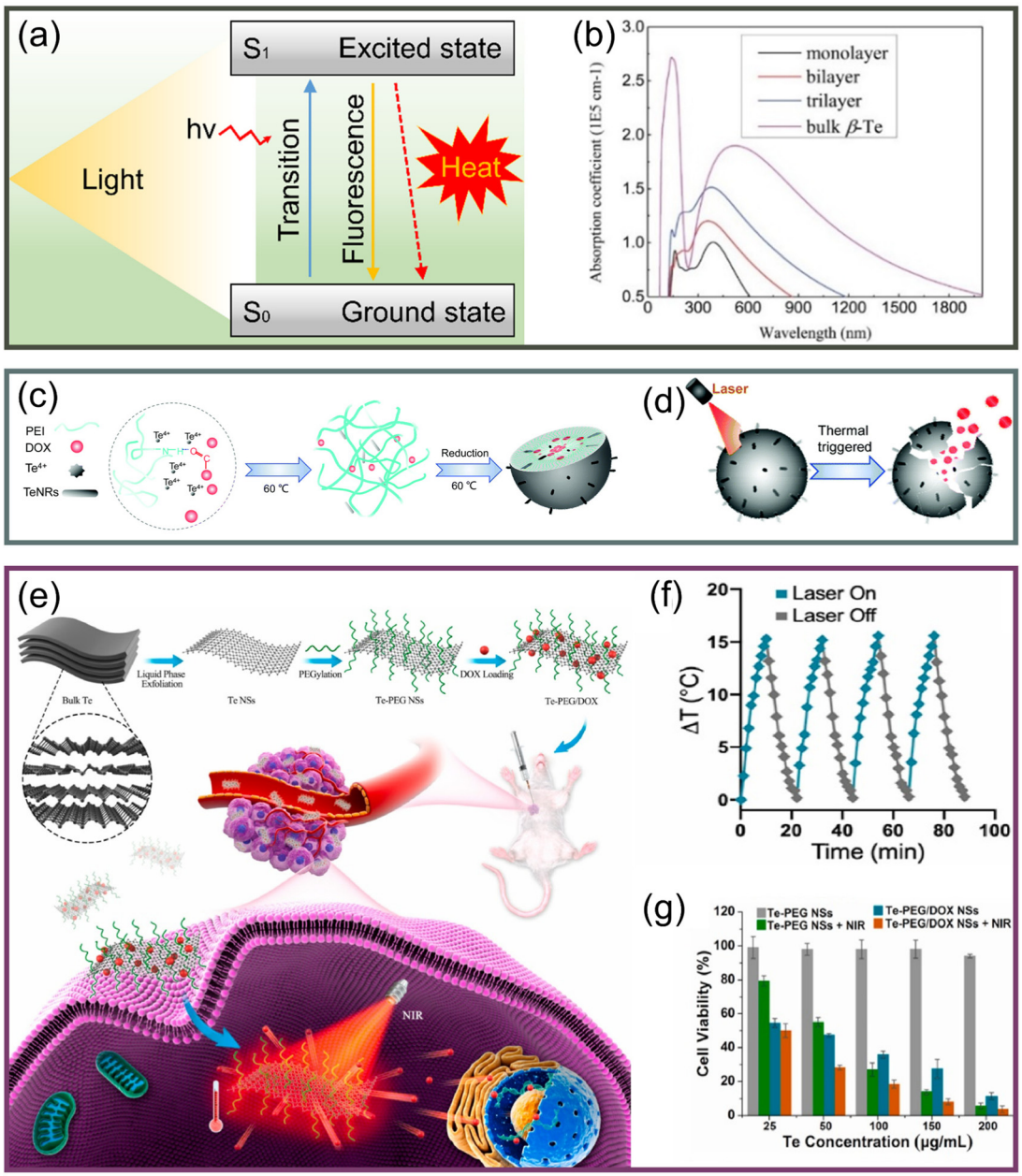

Fig. 6 (a) Schematic of the generation and relaxation of electron–hole pairs due to the absorption of photon energy by nanoparticles and the realization of the photothermal effect. (b) Strong light absorption of Te from UV to visible.[37] Copyright 2017, IOP Publishing. (c) Schematic diagram of DOX/PEI@TeNPs formation process.[112] (d) Light-controlled release mechanism of DOX/PEI@TeNPs.[112] Copyright 2021, Royal Society of Chemistry. (e) Schematic diagram of synthesis and cancer therapy of Te–PEG-NSs.[97] (f) Stability of Te–PEG-NSs in the heating–cooling cycle process.[97] (g) Relative survival rate of 4T1 cells incubated for 24 hours with different treatments.[97] Copyright 2021, Elsevier.

hypoxia condition of tumor tissue, which greatly improved the effect of phototherapy''. Fan *et al.*[119] assembled a multilayer structure comprising a Te-containing polymer (Fig. 7b), indocyanine green, and poly(styrenesulfonate) layer-by-layer. Under laser irradiation, the generated ROS could damage cancer cells and oxidize Te to generate the Te═O group to achieve the controlled release, which provided an interesting insight into Te nanomaterials in phototherapy.

Lin and colleagues further verified the application of 2D tellurene materials in PDT.[23] They synthesized Te nanosheets through LPE and functionalized them with glutathione (GSH) to improve their stability and biocompatibility (Fig. 8a). Fig. 8b shows the strong light absorption of the Te nanosheets@GSH. The change of the trilinear signal in Fig. 8c confirmed the ability of the Te nanosheets@GSH to produce $^1O_2$. Then, dichlorofluorescin-diacetate (DCFH-DA) was used to observe the production of ROS. DCFH-DA is non-fluorescent, but it can be oxidized by ROS and show green fluorescence.[121] The cells incubated with Te nanosheets@GSH had almost no fluorescence, while, after 670 nm light irradiation, they exhibited

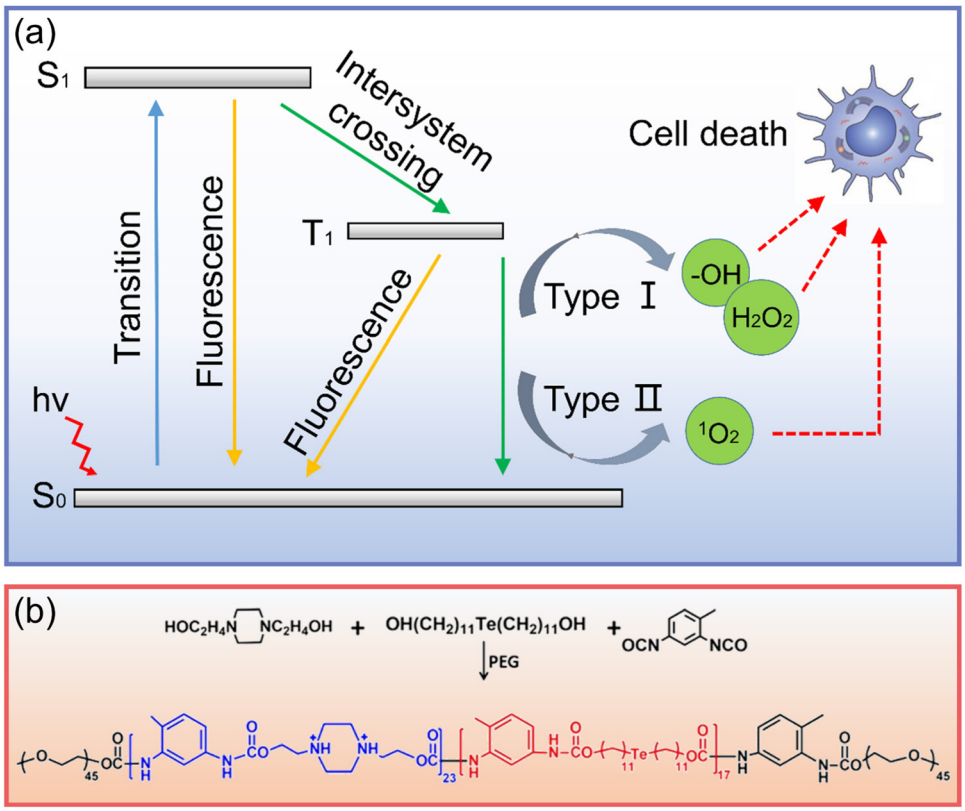

Fig. 7 (a) Schematic diagram of PDT anticancer process (S_0: ground state, S_1: singlet excited state, T_1: excited triplet state). (b) Synthesis of Te-containing polymer.[119] Copyright 2016, American Chemical Society.

strong green fluorescence, as shown in Fig. 8d. Further, from Fig. 8e, the absorption peak intensity of 1,3-diphenylisobenzofuran (DPBF)[122] at 410 nm gradually decreased with an increase in illumination time, which also confirmed that the Te nanosheets@GSH produced ROS under light. *In vitro* experiments, as shown in Fig. 8g, showed that the cell survival rate did not change significantly under dark conditions, while it decreased with an increase in Te nanosheets@GSH concentration under light, which proved that the production of ROS was sufficient to kill cancer cells. The tumor growth of mice was observed after different treatment methods (Fig. 8f and h). The tumor growth of mice treated with Te nanosheets@GSH and light was significantly inhibited, and the tumor tissue was seriously damaged, as shown in Fig. 8i. Both *in vivo* and *in vitro* results showed that 2D tellurene can be used as an attractive photosensitizer for PDT and has broad prospects in biomedical applications.

A 2D Bi/BiO_X lateral nano-heterostructure with similar structure to tellurene was shown to exhibit effective tumor ablation caused by ROS at 660 nm,[123] and antimonene realized PDT under 660 nm and PTT under 808 nm,[124] Jiang *et al.*[63] found that Te nanomaterials exhibit photodynamic effects at 473, 660, and 808 nm, which lays a good foundation of Te nanomaterials to be used for PDT in NIR region to achieve deeper penetration depths.

3.2.3 Photo-triggered molecule delivery. As a new idea, photo-triggered molecule delivery has been widely studied.[125] After a nanoplatform loaded with drug molecules targets the focus area, under the control of a laser, photosensitive nanomaterials will undergo photochemical reaction and break their original stable state, strictly controlling the targeted release of loaded molecules to ensure an effective therapeutic effect.[126] Duan *et al.*[112] realized a Te nanosystem for photo-triggered drug delivery by encapsulating chemotherapy drug DOX and modified it into regular nanospheres. Under the irradiation of an NIR laser, the Te nanomaterials were excited, resulting in the destruction of the nanostructures, which realized the release of the encapsulated chemotherapy drugs. Therefore, with light-controlled Te nanomaterials, it is possible to load chemotherapy and radiotherapy drugs and other potential anticancer nanomaterials, which also provides additional ideas for multi-mode synergistic cancer treatment *via* Te nanomaterials.

3.2.4 Synergetic anticancer application. PTT and PDT are the two main treatment methods of phototherapy. PTT uses the heat generated by an excited photothermal agent to ablate the tumor, but temperatures that are too high may lead to the overexpression of heat-shock proteins, resulting in incomplete apoptosis and tumor recurrence. PDT can produce highly toxic ROS to kill cancer cells. However, due to the vigorous metabolism of dense tumor sites, cells are mostly in a hypoxic state, which indirectly limits the production of ROS and becomes a major obstacle to PDT. Interestingly, the synergetic treatment of PTT and PDT can achieve a significant enhancing

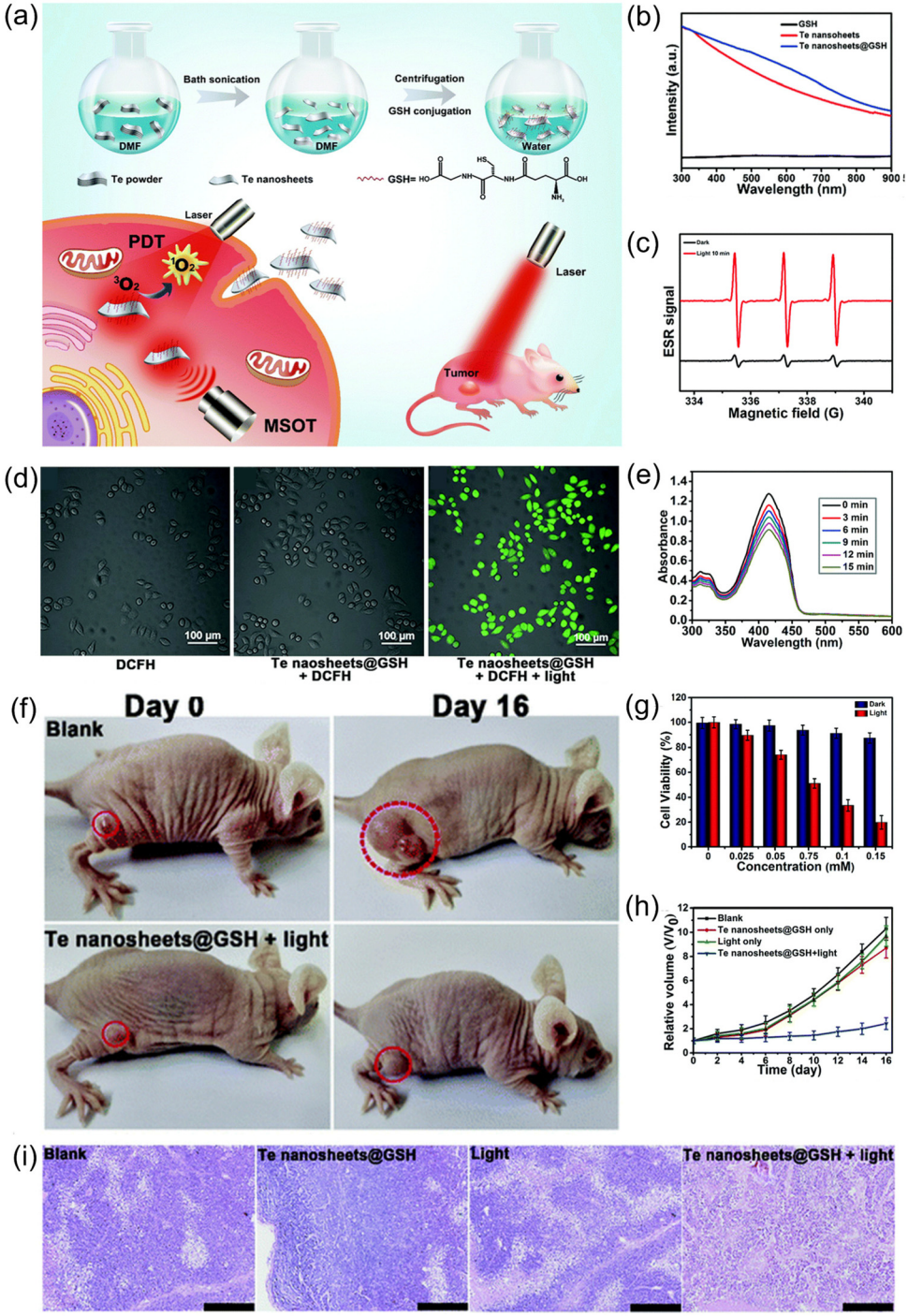

Fig. 8 (a) Schematic diagram of preparation process of Te nanosheets@GSH and their potential applications.[23] (b) UV-Vis absorption spectra of Te nanosheets@GSH, Te nanosheets, and GSH.[23] (c) ESR signal diagram of Te nanosheets in the presence of TEM under light and dark conditions.[23] (d) Merged confocal fluorescence microscopy images of HeLa cells incubated with DCFH, Te nanosheets@GSH + DCFH, and Te nanosheets@GSH + DCFH + light.[23] (Scale bar = 100 μm) (e) UV-Vis absorption spectra of DPBF probe molecules with increasing radiation time.[23] (f) Tumor growth in mice after treatment with a blank and Te nanosheets@GSH + light at Day 0 and Day 16.[23] (g) Cell viability at different concentrations of Te nanosheets@GSH under dark and light conditions.[23] (h) Changes in tumor volume in four groups under different treatment conditions.[23] (i) H&E staining histological images of tumor sections after four groups of different treatment conditions.[23] (Scale bar = 200 μm) (Laser wavelength = 670 nm, 160 mW cm^{-2}) Copyright 2018, Royal Society of Chemistry.

effect.[89,127] Studies have shown that PTT leads to an increase in the local temperature and blood flow velocity of tumors,[128,129] which promotes material exchange and can continuously supplement oxygen to tumor tissue to realize continuous PDT, which makes synergistic therapy significantly advantageous.

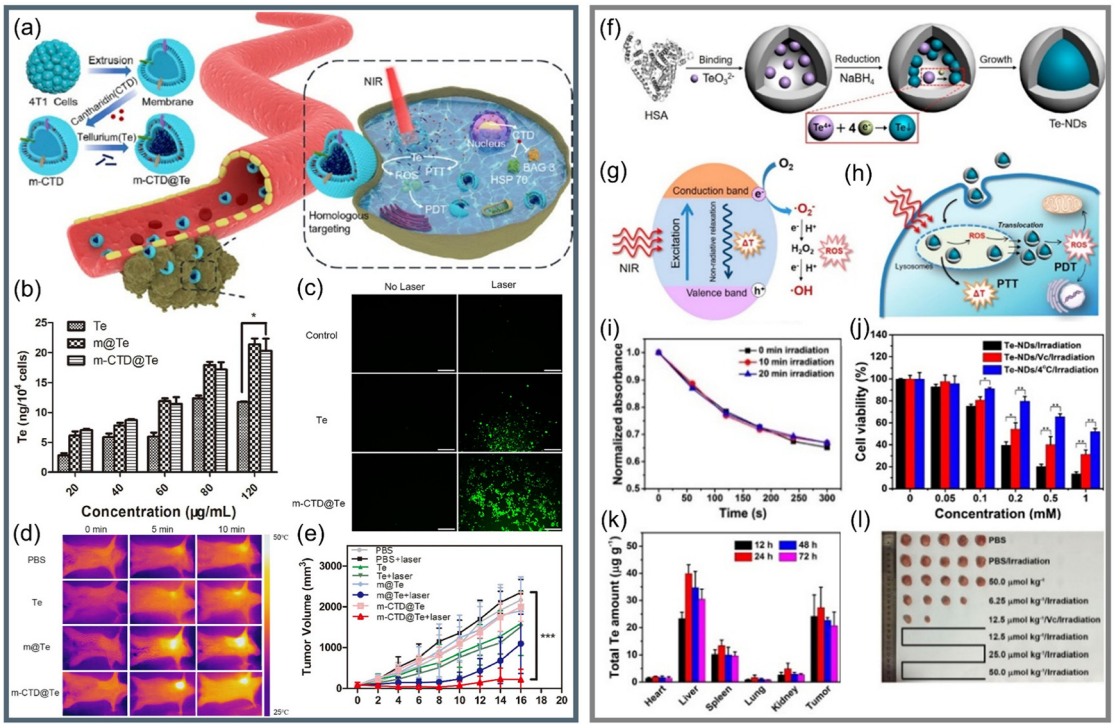

Fig. 9 (a) Schematic diagram of preparation of m-CTD@Te and synergetic anticancer applications.[121] (b) Content of Te in 4T1 cells after treatment with different groups by Te, m@Te, and m-CTD@Te.[121] (c) Exploring of the ability of Te and m-CTD@Te to generate ROS through DCFH-DA.[121] (d) Real-time thermography of mice after intravenous injection of Te, m@Te, m-CTD@Te, and PBS.[121] (e) Change curve of tumor volume during 16 days of treatment (Laser wavelength = 808 nm, 1.0 W cm^{-2}).[121] Copyright 2020, Elsevier. (f) Schematic diagram of bifunctional Te-NDs synthesis with HSA as a nano reactor.[55] (g) and (h) show the photothermal effect and ROS generation of Te-NDs to realize PTT/PDT synergistic treatment, respectively.[55] (i) Relationship between the standard absorption of DPBF and Te-NDs irradiation time for 0 min, 10 min, and 20 min.[55] (j) A chart comparing the cell survival rate of the three groups.[55] (k) The total Te content of several main tissues after treated by Te-NDs for different periods of time.[55] (l) Pictures of mice tumors after treated for 30 days (Laser wavelength = 785 nm, 1.5 W cm^{-2}).[55] Copyright 2017, American Chemical Society.

As an attractive candidate, Te nanomaterials can not only produce PTT through the generation and relaxation of electron–hole pairs but also trigger the generation of ROS through the reaction between excitons and water/oxygen to realize PTT/PDT synergetic therapy.[130–132] It has been reported that Te nanomaterials have great potential in cancer synergetic therapy.[55,92,121] Guo *et al.*[121] loaded the chemotherapeutic drug cantharidin and Te nanoparticles into the 4T1 cell membrane with a homologous targeting ability to develop cancer-cell-camouflaged nano therapeutic agent m-CTD@Te (Fig. 9a). As shown in Fig. 9b, compared with bare Te, the Te nanomaterials coated with cell membrane showed higher cell uptake, which had decisive significance for the realization of targeted anticancer therapy; after 808 nm laser treatment, the generation of ROS was verified, as seen in Fig. 9c. The infrared thermal imaging photographs in Fig. 9d clearly show the higher photothermal effect of the tumor area than the normal area, confirming the targeting ability of m-CTD@Te *in vivo*. At the same time, the significant difference in tumor volume (Fig. 9e) also proved that m-CTD@Te realized high-efficiency PDT/PTT anticancer effects through the single light source.

Yang *et al.*[55] used human serum albumin (HSA) as a nano reactor to synthesize bifunctional Te nanodots (Te-NDs) to realize PTT/PDT synergetic therapy under the irradiation of a single 785 nm light, as shown in Fig. 9f–h. Apart from the known photothermal effect, DPBF was used to capture ROS, and the Te-NDs still maintained the ability to produce ROS even after 10 and 20 min of irradiation (Fig. 9i). In order to verify the synergetic effect, they used a scavenger of ROS, vitamin C, to inhibit the photodynamic effect, and the environment at 4 °C inhibited the photothermal effect; the comparison of cell survival rates of the three groups in Fig. 9j proves the synergetic PTT/PDT effect. Due to the EPR effect and the tumor accumulation capacity of albumin,[133,134] the Te-NDs would mainly distribute in tumor and liver areas (Fig. 9k), and the significant tumor ablation in Fig. 9l proves phototherapeutic ability of Te nanomaterials.

Under extensive laser irradiation, because Ru can catalyze peroxide to produce oxygen to improve PDT efficiency, spotted Ru–Te hollow nanorods were able to achieve high-efficiency synergetic PTT/PDT for anoxic pancreatic cancer,[63] which provided a reference for the fusion of Te nanomaterials and other materials to realize multifunctional anticancer modes. Li *et al.*[135] prepared Te nanorods using peptides as nano reactors to achieve efficient PTT/sonodynamic therapy. The presence of peptides and HSA ensured that the Te nanomaterials had high dispersion and stability, avoiding complex modification. Huang *et al.*[136] explored a combination of triangular nanocrystals in

radiotherapy and immunotherapy, which provided a new idea for phototherapy combined with immunotherapy *via* Te nanomaterials.

3.3 Breakthrough of Te nanomaterials in cancer treatment

As a chiral-chain-structure semiconductor material, Te has the outstanding advantage of a high light absorption and can realize PTT and PDT simultaneously under the excitation of a single light source, which greatly inspires and promotes the realization of efficient and synergistic cancer treatment.

Unfortunately, the biggest threat of Te nanomaterials to organisms is that we have a limited understanding of their metabolism, transformation and possible toxicity *in vivo*.[137] In addition, Te has poor compatibility in organisms and may have potential toxicity to the human body. How to improve the biocompatibility and reduce the biological toxicity of Te nanomaterials are questions that must be solved urgently. Here, based on previous studies, we propose the surface modification and size control of Te nanomaterials to affect their metabolic behavior in organisms with the hope to achieve a breakthrough of Te nanomaterials in cancer treatment through more research.

3.3.1 Surface modification. Many nanomaterials will aggregate in organisms due to their hydrophobicity, which hinders their biomedical applications.[138] In order to ensure their good biocompatibility and stability in organisms, their exterior will usually be modified by hydrophilic groups or coated proteins or biofilms. Lin *et al.*[23] modified the surface of tellurene by GSH and incubated with HeLa cells for 24 hours, where there was no significant change in cell survival, as shown in Fig. 10a. Huang *et al.*[139] used the polysaccharide–protein complex as the end cap for Te nanorods, which significantly improved the stability and biocompatibility of the material. Protein networks provide the possibility to achieve a full coating; among them, bovine serum albumin (BSA) is also widely used in biomedical research due to its good biocompatibility.[140] Zhou *et al.*[141] modified Te nanoparticles with BSA to obtain good biocompatibility. Compared with the coating process, Yang *et al.*[55] directly used HSA as nano reactors to prepare Te nanoparticles, which greatly simplified the preparation process. The same idea was reflected in the work of Li *et al.*,[135] who used polypeptides and demonstrated the biosafety of Te nanomaterials through the survival of 4T1 cells, as shown in Fig. 10b. These modification methods provide an effective strategy for improving the stability and biocompatibility of Te nanomaterials.

Chen *et al.*[83] developed a TeSe nano-heterojunction structure (Fig. 5e) comprising a Se coating covering a Te nanosheet. Mixing with SMMC-7721 cells, it was observed that the cell survival rate under pure Te decreased sharply at a concentration of 100 ppm, while the Te nanomaterials encapsulated by Se were non-toxic at a concentration of 400 ppm, as shown in Fig. 10d. The consistency of tissue structures in organ-slice images in Fig. 10c and no significant changes in body weight, as shown in Fig. 10e, demonstrated that Te nanomaterials coated with Se had better biocompatibility. A similar work with Ru–Te hollow nanorods also proved the feasibility of this program.[63]

Therefore, it is safe to conclude that reasonable modification of Te nanomaterials is a breakthrough idea to reduce their toxicity, improve their biocompatibility, and ensure their therapeutic effect, which is significant for their application in biomedical field. In addition, ligands with a targeting effect (such as towards 4T1 cell membranes[121]) can be employed to improve the specific recognition ability of materials, so as to improve their targeting ability in tumor therapy.

3.3.2 Size and metabolism. In addition to surface modification, size-control strategies are another breakthrough. Many inorganic nanoparticles remain in organisms for a long time and are difficult to be removed, which leads to potential toxicity and hinders their application in the biomedical field.[20] For cancer therapy, we expect that inorganic nanoparticles can effectively damage cancer cells and be removed from the body as soon as possible after treatment. Among them, renal excretion is the preferred and ideal pathway.

Ultrathin Te nanosheets prepared by Pan *et al.*[97] could still maintain a cellular survival rate of 90% after incubation with cancer cells (4T1) and normal cells (L929 fibroblast cells) for 24 hours, as shown in Fig. 10f and g, indicating that they had very low biological toxicity. Te NDs synthesized by Yang *et al.*[55] had an ultra-small size (<10 nm), which was conducive to renal excretion.[20,142] In order to explore the excretion and clearance behavior of Te-NDs *in vivo*, the elimination ability was evaluated by monitoring the distribution of Te in heart, liver, spleen, lung, and kidney over 28 days, as shown in Fig. 10h. It was clearly observed that after the third day, the content of Te in each tissue decreased dramatically. In addition, the markers of liver and kidney function (ALP/ALT/AST and urea) had no significant difference compared with the original levels after being injected for 28 days, as shown in Fig. 10i and j. It was confirmed that Te-NDs had no obvious toxicity to normal tissues, and that their ultra-small size possibly led them to be excreted from normal tissues through the kidney. This work provided a breakthrough idea for the study of long-term retention and toxicity of Te nanomaterials *in vivo* and significantly enlightens the study of inorganic phototherapeutic nanomaterials, which has great significance for their clinical application.

4. Summary and prospective

This review summarizes the synthesis methods, properties, and mechanism of Te nanomaterials, as well as their applications in cancer phototherapy, and it puts forward some breakthroughs in the direction of cancer phototherapy with regards to possible biocompatibility and potential biological toxicity. We hope to fully utilize the advantageously high light absorption and phototherapeutic potential of Te nanomaterials, so as to promote their application in biomedicine.

At present, studies have shown the application of Te nanomaterials in the biological field, as well as their fascinating characteristics, such as high carrier mobility, strong light absorption, and PTT/PDT synergetic therapy excited by a single light source, making them outstanding in tumor phototherapy.

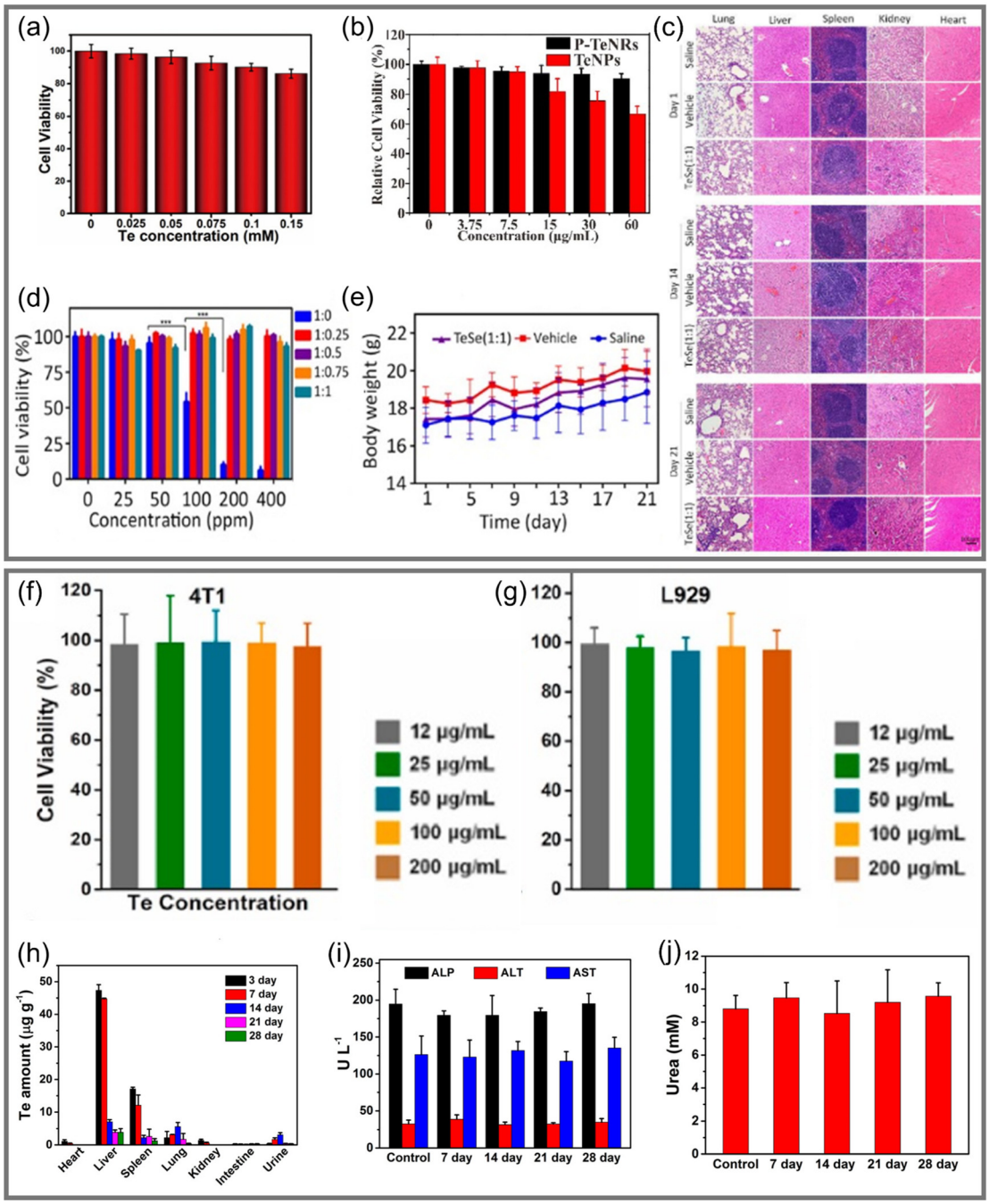

Fig. 10 (a) Relative viability of HeLa cells after incubated by Te nanosheets@GSH for 24 hours.[23] Copyright 2018, Royal Society of Chemistry. (b) Relative viability of 4T1 cells after incubated with Te nanomaterials.[135] Copyright 2021, Elsevier. (c) H&E slice image of different tissues treated by several groups at days 1, 14, and 21.[83] (Scale bar = 100 μm.) (d) Survival rate of SMMC-7721 cancer cells treated with nanomaterials under different Te : Se ratios.[83] (e) Body weight changes of mice treated in different groups from day 1 to day 21, with 5 mice in each group.[83] Copyright 2020, American Association for the Advancement of Science. (f) and (g) are the relative viability of 4T1 cells and L929 after incubated with ultrathin Te nanosheets for 24 hours, respectively.[97] Copyright 2021, Elsevier. (h) Distribution of Te in various mouse tissues that were treated with 50.0 μmol kg^{-1} Te over 28 days.[55] (i) Levels of ALP, ALT, and AST in blood of mice in a control group and mice injected with 50.0 μmol kg^{-1} Te at different times.[55] (j) Level of urea in blood of mice in a control group and mice injected with 50.0 μmol kg^{-1} Te at different times.[55] Copyright 2017, American Chemical Society.

Especially, tellurene can control/accelerate the release of drugs from the delivery platform due to the NIR photothermal effect, owing to the unique ultra-high surface area to volume ratio and ultra-thin 2D nanosheet structure. These prominent merits of Te nanomaterials make them very likely to realize the synergistic treatment of tumor radio/chemo/phototherapy, indicating their great potential as effective anti-cancer agents.

However, there has been little research on Te nanomaterials in the biomedical field, which indicates many gaps and great challenges; the harsh conditions required by PVD, such as the high vacuum environment, and the difficulty in size-control of LPE are factors that limit their development. Therefore, much exploration is still needed to discover simple and efficient methods to synthesize Te nanomaterials with uniform size and large scale. In addition, as we all know, the controversial problem of some nano biomaterials is the biocompatibility of the as-prepared materials. The production of Te nanomaterials usually involves the use of toxic reactants and organic solvents, which limits their application in the clinical field. In the process of material preparation, a solvent with good biocompatibility and high hydrophilicity can be used as the reaction base, which can greatly improve the biocompatibility of the final product. Moreover, surface modification and size control to improve biocompatibility, produce a small immune response, and reduce or even eliminate biological toxicity are the major breakthrough points of Te nanomaterials in cancer treatment.

In addition, the excellent performance of Te nanomaterials in phototherapy such as fast response to NIR laser and good photothermal performance makes it possible for more diseases. For example, in cardiovascular and cerebrovascular diseases, the warm photothermal effect through controlling the dose of Te nanomaterials can improve the water solubility of blood lipids and reduce blood viscosity, meanwhile, it can also soften blood vessels to accelerate blood circulation. What's more, the layered structure of tellurene has high drug loading capacity, and has promising approach in targeted drug delivery after reasonable modification. We expect that Te nanomaterials can maximize the therapeutic effect and minimize side effects. Although there have been some preliminary theoretical proofs and experimental studies on the application of Te nanomaterials in the biological field, the interaction between Te and organisms, metabolism in organisms, and short-term and long-term biological toxicity still call for in-depth exploration. Therefore, more effort must be exerted to realize the development and breakthrough of Te nanomaterials in the biomedical field. We maintain an optimistic point of view that there will be more opportunities for Te nanomaterials in the near future.

Abbreviations

EPR	Enhanced permeation and retention
2D	Two-dimensional
PDT	Photodynamic therapy
PTT	Photothermal therapy
Te	Tellurium
NIR	Near-infrared
1D	One-dimensional
PVD	Physical vapor deposition
MBE	Molecular beam epitaxy
PLD	Pulsed laser deposition
vdWE	van der Waals epitaxy
LPE	Liquid-phase exfoliation
NMP	*N*-Methylpyrrolidinone
PVP	Polyvinylpyrrolidone
ROS	Reactive oxygen species
UV	Ultraviolet light
DOX	Doxorubicin hydrochloride
PEG	Polyethylene glycol
$^1O_2$	Singlet oxygen
GSH	Glutathione
DCFH-DA	Dichlorofluorescin-diacetate
DPBF	1,3-Diphenylisobenzofuran
HSA	Human serum albumin
Te-NDs	Te nanodots
BSA	Bovine serum albumin
ALP	Alkaline phosphatase
ALT	Alanine aminotransferase
AST	Aspartate aminotransferase

Conflicts of interest

The authors declare that they have no known competing financial interests or personal relationships that could have appeared to influence the work reported in this paper.

Acknowledgements

The authors acknowledge financial support from the National Natural Science Foundation of China (Grant No. 52101287 and U1806219). The Special Funding also supports this work in the Project of the Qilu Young Scholar Program of Shandong University.

References

1 W. P. Fan, B. Yung, P. Huang and X. Y. Chen, *Chem. Rev.*, 2017, **117**, 13566–13638.
2 The Lancet, *Lancet*, 2018, **392**, 985.
3 Z. Cheng, M. Y. Li, R. Dey and Y. H. Chen, *J. Hematol. Oncol.*, 2021, **14**, 27.
4 X. Yi, K. Yang, C. Liang, X. Y. Zhong, P. Ning, G. S. Song, D. L. Wang, C. C. Ge, C. Y. Chen, Z. F. Chai and Z. Liu, *Adv. Funct. Mater.*, 2015, **25**, 4689–4699.
5 C. Early Breast Canc Trialists, *Lancet*, 2011, **378**, 1707–1716.
6 Z. J. Zhang, J. Wang and C. H. Chen, *Adv. Mater.*, 2013, **25**, 3869–3880.
7 P. Y. Chen, Y. C. Ma, Z. Zheng, C. F. Wu, Y. C. Wang and G. L. Liang, *Nat. Commun.*, 2019, **10**, 1192.
8 Q. Wang, Y. N. Dai, J. Z. Xu, J. Cai, X. R. Niu, L. Zhang, R. F. Chen, Q. M. Shen, W. Huang and Q. L. Fan, *Adv. Funct. Mater.*, 2019, **29**, 12.
9 J. Nam, S. Son, L. J. Ochyl, R. Kuai, A. Schwendeman and J. J. Moon, *Nat. Commun.*, 2018, **9**, 13.
10 S. L. Gai, G. X. Yang, P. P. Yang, F. He, J. Lin, D. Y. Jin and B. G. Xing, *Nano Today*, 2018, **19**, 146–187.

11 D. M. Sun, X. Y. Zhuang, S. Q. Zhang, Z. B. Deng, W. Grizzle, D. Miller and H. G. Zhang, *Adv. Drug Delivery Rev.*, 2013, **65**, 342–347.
12 W. W. Qin, G. Huang, Z. G. Chen and Y. Q. Zhang, *Front. Pharmacol.*, 2017, **8**, 15.
13 A. Y. Lin, J. K. Young, A. V. Nixon and R. A. Drezek, *Small*, 2014, **10**, 3246–3251.
14 N. Karousis, I. Suarez-Martinez, C. P. Ewels and N. Tagmatarchis, *Chem. Rev.*, 2016, **116**, 4850–4883.
15 H. P. Cui, K. Zheng, L. Q. Tao, J. B. Yu, X. Y. Zhu, X. D. Li and X. P. Chen, *IEEE Electron Device Lett.*, 2019, **40**, 1522–1525.
16 X. Y. Yang, G. Y. Liu, Y. H. Shi, W. Huang, J. J. Shao and X. C. Dong, *Nanotechnology*, 2018, **29**, 15.
17 W. Tao, N. Kong, X. Y. Ji, Y. P. Zhang, A. Sharma, J. Ouyang, B. W. Qi, J. Q. Wang, N. Xie, C. Kang, H. Zhang, O. C. Farokhzad and J. S. Kim, *Chem. Soc. Rev.*, 2019, **48**, 2891–2912.
18 H. Lin, X. G. Wang, L. D. Yu, Y. Chen and J. L. Shi, *Nano Lett.*, 2017, **17**, 384–391.
19 Y. B. Li, W. Lu, Q. A. Huang, M. A. Huang, C. Li and W. Chen, *Nanomedicine*, 2010, **5**, 1161–1171.
20 H. Kang, S. Mintri, A. V. Menon, H. Y. Lee, H. S. Choi and J. Kim, *Nanoscale*, 2015, **7**, 18848–18862.
21 W. Tao, X. Y. Ji, X. B. Zhu, L. Li, J. Q. Wang, Y. Zhang, P. E. Saw, W. L. Li, N. Kong, M. A. Islam, T. Gan, X. W. Zeng, H. Zhang, M. Mahmoudi, G. J. Tearney and O. C. Farokhzad, *Adv. Mater.*, 2018, **30**, 11.
22 W. Tao, X. Y. Ji, X. D. Xu, M. A. Islam, Z. J. Li, S. Chen, P. E. Saw, H. Zhang, Z. Bharwani, Z. L. Guo, J. J. Shi and O. C. Farokhzad, *Angew. Chem., Int. Ed.*, 2017, **56**, 11896–11900.
23 Y. Lin, Y. Wu, R. Wang, G. Tao, P. F. Luo, X. Lin, G. M. Huang, J. Li and H. H. Yang, *Chem. Commun.*, 2018, **54**, 8579–8582.
24 S. J. Gao, Y. X. Wang, R. X. Wang and W. Z. Wu, *Semicond. Sci. Technol.*, 2017, **32**, 9.
25 Y. Wang, C. C. Xiao, M. G. Chen, C. Q. Hu, J. D. Zou, C. Wu, J. Z. Jiang, S. Y. A. Yang, Y. H. Lu and W. Ji, *Mater. Horiz.*, 2018, **5**, 521–528.
26 S. Deckoff-Jones, Y. X. Wang, H. T. Lin, W. Z. Wu and J. J. Hu, *ACS Photonics*, 2019, **6**, 1632–1638.
27 W. Z. Wu, G. Qiu, Y. X. Wang, R. X. Wang and P. D. Ye, *Chem. Soc. Rev.*, 2018, **47**, 7203–7212.
28 J. S. Qiao, Y. H. Pan, F. Yang, C. Wang, Y. Chai and W. Ji, *Sci. Bull.*, 2018, **63**, 159–168.
29 S. Berweger, G. Qiu, Y. X. Wang, B. Pollard, K. L. Genter, R. Tyrrell-Ead, T. M. Wallis, W. Z. Wu, P. D. Ye and P. Kabos, *Nano Lett.*, 2019, **19**, 1289–1294.
30 G. Qiu, Y. X. Wang, Y. F. Nie, Y. P. Zheng, K. Cho, W. Z. Wu and P. D. D. Ye, *Nano Lett.*, 2018, **18**, 5760–5767.
31 S. Sharma, N. Singh and U. Schwingenschlogl, *ACS Appl. Energy Mater.*, 2018, **1**, 1950–1954.
32 K. K. Wen, L. F. Wu, X. X. Wu, Y. Lu, T. Duan, H. Ma, A. D. Peng, Q. Q. Shi and H. Huang, *Angew. Chem., Int. Ed.*, 2020, **59**, 12756–12761.
33 B. Mayers and Y. N. Xia, *Adv. Mater.*, 2002, **14**, 279–282.
34 B. Mayers and Y. N. Xia, *J. Mater. Chem.*, 2002, **12**, 1875–1881.
35 Y. X. Wang, G. Qiu, R. X. Wang, S. Y. Huang, Q. X. Wang, Y. Y. Liu, Y. C. Du, W. A. Goddard, M. J. Kim, X. F. Xu, P. D. Ye and W. Z. Wu, *Nat. Electron.*, 2018, **1**, 228–236.
36 Z. B. Gao, G. Liu and J. Ren, *ACS Appl. Mater. Interfaces*, 2018, **10**, 40702–40709.
37 B. Z. Wu, X. H. Liu, J. R. Yin and H. Lee, *Mater. Res. Express*, 2017, **4**, 8.
38 C. Wang, X. Y. Zhou, J. S. Qiao, L. W. Zhou, X. H. Kong, Y. H. Pan, Z. H. Cheng, Y. Chai and W. Ji, *Nanoscale*, 2018, **10**, 22263–22269.
39 X. H. Wang, D. W. Wang, A. J. Yang, N. Koratkar, J. F. Chu, P. L. Lv and M. Z. Rong, *Phys. Chem. Chem. Phys.*, 2018, **20**, 4058–4066.
40 J. H. Yan, X. Y. Zhang, Y. Y. Pan, J. Z. Li, B. W. Shi, S. Q. Liu, J. Yang, Z. G. Song, H. Zhang, M. Ye, R. G. Quhe, Y. Y. Wang, J. B. Yang, F. Pan and J. Lu, *J. Mater. Chem. C*, 2018, **6**, 6153–6163.
41 R. J. Turner, R. Borghese and D. Zannoni, *Biotechnol. Adv.*, 2012, **30**, 954–963.
42 M. M. Luo, T. J. Fan, Y. Zhou, H. Zhang and L. Mei, *Adv. Funct. Mater.*, 2019, **29**, 19.
43 H. J. Guo, K. Zheng, H. P. Cui, J. B. Yu, L. Q. Tao, X. D. Li, C. R. Liao, L. Xie and X. P. Chen, *Appl. Surf. Sci.*, 2020, **532**, 7.
44 Z. B. Gao, F. Tao and J. Ren, *Nanoscale*, 2018, **10**, 12997–13003.
45 J. L. Chen, Y. W. Dai, Y. Q. Ma, X. Q. Dai, W. K. Ho and M. H. Xie, *Nanoscale*, 2017, **9**, 15945–15948.
46 Z. He, Y. Yang, J. W. Liu and S. H. Yu, *Chem. Soc. Rev.*, 2017, **46**, 2732–2753.
47 M. Amani, C. L. Tan, G. Zhang, C. S. Zhao, J. Bullock, X. H. Song, H. Kim, V. R. Shrestha, Y. Gao, K. B. Crozier, M. Scott and A. Javey, *ACS Nano*, 2018, **12**, 7253–7263.
48 Y. N. Xia, W. Y. Li, C. M. Cobley, J. Y. Chen, X. H. Xia, Q. Zhang, M. X. Yang, E. C. Cho and P. K. Brown, *Acc. Chem. Res.*, 2011, **44**, 914–924.
49 L. Zhang, Z. X. Xie and J. L. Gong, *Chem. Soc. Rev.*, 2016, **45**, 3916–3934.
50 Z. Shi, R. Cao, K. Khan, K. Tareen Ayesha, X. Liu, W. Liang, Y. Zhang, C. Ma, Z. Guo, X. Luo and H. Zhang, *Nano-Micro Lett.*, 2020, **12**, 99.
51 J. M. Pietryga, Y. S. Park, J. H. Lim, A. F. Fidler, W. K. Bae, S. Brovelli and V. I. Klimov, *Chem. Rev.*, 2016, **116**, 10513–10622.
52 Y. H. Liu, H. Huang, W. J. Cao, B. D. Mao, Y. Liu and Z. H. Kang, *Mater. Chem. Front.*, 2020, **4**, 1586–1613.
53 M. Tuerhong, Y. Xu and X. B. Yin, *Chin. J. Anal. Chem.*, 2017, **45**, 139–149.
54 H. Li, Z. Kang, Y. Liu and S.-T. Lee, *J. Mater. Chem.*, 2012, **22**, 24230–24253.
55 T. Yang, H. T. Ke, Q. L. Wang, Y. A. Tang, Y. B. Deng, H. Yang, X. L. Yang, P. Yang, D. S. Ling, C. Y. Chen, Y. L. Zhao, H. Wu and H. B. Chen, *ACS Nano*, 2017, **11**, 10012–10024.
56 W. D. He, A. Krejci, J. H. Lin, M. E. Osmulski and J. H. Dickerson, *Nanoscale*, 2011, **3**, 1523–1525.
57 J. K. Qin, P. Y. Liao, M. W. Si, S. Y. Gao, G. Qiu, J. Jian, Q. X. Wang, S. Q. Zhang, S. Y. Huang, A. Charnas,

Y. X. Wang, M. J. Kim, W. Z. Wu, X. F. Xu, H. Y. Wang, L. Yang, Y. K. Yap and P. D. D. Ye, *Nat. Electron.*, 2020, **3**, 141–147.
58 O. Erol, I. Uyan, M. Hatip, C. Yilmaz, A. B. Tekinay and M. O. Guler, *Nanomedicine*, 2018, **14**, 2433–2454.
59 M. F. Pantano and I. Kuljanishvili, *Nano Express*, 2020, **1**, 25.
60 B. Y. Geng, Y. Lin, X. S. Peng, G. W. Meng and L. D. Zhang, *Nanotechnology*, 2003, **14**, 983–986.
61 M. Safdar, X. Y. Zhan, M. T. Niu, M. Mirza, Q. Zhao, Z. X. Wang, J. P. Zhang, L. F. Sun and J. He, *Nanotechnology*, 2013, **24**, 8.
62 P. Bhol, S. Swain, S. Jena, K. Bhatte, C. S. Rout, M. Saxena, A. H. Jadhav and A. K. Samal, *ACS Appl. Nano Mater.*, 2021, **4**, 9008–9021.
63 S. Kang, Y. G. Gil, D. H. Min and H. Jang, *ACS Nano*, 2020, **14**, 4383–4394.
64 Q. S. Wang, M. Safdar, K. Xu, M. Mirza, Z. X. Wang and J. He, *ACS Nano*, 2014, **8**, 7497–7505.
65 C. D. Zhang, A. Johnson, C. L. Hsu, L. J. Li and C. K. Shih, *Nano Lett.*, 2014, **14**, 2443–2447.
66 A. Apte, E. Bianco, A. Krishnamoorthy, S. Yazdi, R. Rao, N. Glavin, H. Kumazoe, V. Varshney, A. Roy, F. Shimojo, E. Ringe, R. K. Kalia, A. Nakano, C. S. Tiwari, P. Vashishta, V. Kochat and P. M. Ajayan, *2D Mater.*, 2019, **6**, 9.
67 Z. J. Xie, C. Y. Xing, W. C. Huang, T. J. Fan, Z. J. Li, J. L. Zhao, Y. J. Xiang, Z. N. Guo, J. Q. Li, Z. G. Yang, B. Q. Dong, J. L. Qu, D. Y. Fan and H. Zhang, *Adv. Funct. Mater.*, 2018, **28**, 11.
68 F. Cai, X. Huang, Q. Yang and D. Nagy, *Trans. ASME: J. Eng. Gas Turbines Power*, 2012, **134**, 8.
69 F. Cernuschi, L. Lorenzoni, S. Capelli, C. Guardamagna, M. Karger, R. Vassen, K. von Niessen, N. Markocsan, J. Menuey and C. Giolli, *Wear*, 2011, **271**, 2909–2918.
70 J. H. Yuan, Q. Zhan, Q. Lei, S. Y. Ding and H. Li, *Appl. Surf. Sci.*, 2012, **258**, 6672–6678.
71 D. H. Boone, *Mater. Sci. Technol.*, 1986, **2**, 220–224.
72 M. Kracht, J. Schormann and M. Eickhoff, *J. Cryst. Growth*, 2016, **436**, 87–91.
73 A. Koma, *Thin Solid Films*, 1992, **216**, 72–76.
74 J. P. Ji, X. F. Song, J. Z. Liu, Z. Yan, C. X. Huo, S. L. Zhang, M. Su, L. Liao, W. H. Wang, Z. H. Ni, Y. F. Hao and H. B. Zeng, *Nat. Commun.*, 2016, **7**, 9.
75 X. C. Huang, J. Q. Guan, Z. J. Lin, B. Liu, S. Y. Xing, W. H. Wang and J. D. Guo, *Nano Lett.*, 2017, **17**, 4619–4623.
76 X. G. Gu, Y. Zhao, K. Sun, C. L. Z. Vieira, Z. J. Jia, C. Cui, Z. J. Wang, A. Walsh and S. D. Huang, *Ultrason. Sonochem.*, 2019, **58**, 12.
77 C. Gibaja, D. Rodriguez-San-Miguel, P. Ares, J. Gomez-Herrero, M. Varela, R. Gillen, J. Maultzsch, F. Hauke, A. Hirsch, G. Abellan and F. Zamora, *Angew. Chem., Int. Ed.*, 2016, **55**, 14343–14347.
78 G. W. Liu, J. J. Yuan, T. G. Wu, F. Zhang, F. Xing, W. F. Zhang, H. N. Zhang and S. G. Fu, *IEEE J. Sel. Top. Quantum Electron.*, 2021, **27**, 6.
79 K. Manna, H. N. Huang, W. T. Li, Y. H. Ho and W. H. Chiang, *Chem. Mater.*, 2016, **28**, 7586–7593.
80 J. N. Coleman, M. Lotya, A. O'Neill, S. D. Bergin, P. J. King, U. Khan, K. Young, A. Gaucher, S. De, R. J. Smith, I. V. Shvets, S. K. Arora, G. Stanton, H. Y. Kim, K. Lee, G. T. Kim, G. S. Duesberg, T. Hallam, J. J. Boland, J. J. Wang, J. F. Donegan, J. C. Grunlan, G. Moriarty, A. Shmeliov, R. J. Nicholls, J. M. Perkins, E. M. Grieveson, K. Theuwissen, D. W. McComb, P. D. Nellist and V. Nicolosi, *Science*, 2011, **331**, 568–571.
81 H. Qi, B. Liang and U. Kaiser, *SmartMat*, 2021, **2**, 131–138.
82 Y. C. Du, G. Qiu, Y. X. Wang, M. W. Si, X. F. Xu, W. Z. Wu and P. D. D. Ye, *Nano Lett.*, 2017, **17**, 3965–3973.
83 S. Y. Chen, C. Y. Xing, D. Z. Huang, C. H. Zhou, B. Ding, Z. H. Guo, Z. C. Peng, D. Wang, X. Zhu, S. Z. Liu, Z. Cai, J. Y. Wu, J. Q. Zhao, Z. Z. Wu, Y. H. Zhang, C. Y. Wei, Q. T. Yan, H. Z. Wang, D. Y. Fan, L. P. Liu, H. Zhang and Y. H. Cao, *Sci. Adv.*, 2020, **6**, 11.
84 M. Qiu, D. Wang, H. Huang, T. Yin, W. L. Bao, B. Zhang, Z. J. Xie, N. Xie, Z. Z. Wu, C. C. Ge, Q. Wang, M. Gu, H. L. Kutscher, L. P. Liu, S. Y. Bao, P. N. Prasad and H. Zhang, *Adv. Mater.*, 2021, **33**, 2102562.
85 M. Qiu, Y. H. Duo, W. Y. Liang, Y. L. Yang, B. Zhang, Z. J. Xie, X. L. Yang, G. Q. Wang, N. Xie, G. H. Nie, O. A. Alhartomy, A. A. Alghamdi, S. Wageh, Y. H. Cao and H. Zhang, *Adv. Funct. Mater.*, 2021, **31**, 17.
86 A. Walther and A. H. E. Muller, *Chem. Rev.*, 2013, **113**, 5194–5261.
87 T. D. Schladt, K. Schneider, H. Schild and W. Tremel, *Dalton Trans.*, 2011, **40**, 6315–6343.
88 Y. P. Guo, H. S. Wang, X. Feng, Y. B. Zhao, C. Y. Liang, L. Yang, M. J. Li, Y. G. Zhang and W. Gao, *Nanotechnology*, 2021, **32**, 11.
89 H. J. Zhu, P. H. Cheng, P. Chen and K. Y. Pu, *Biomater. Sci.*, 2018, **6**, 746–765.
90 H. S. Jung, P. Verwilst, A. Sharma, J. Shin, J. L. Sessler and J. S. Kim, *Chem. Soc. Rev.*, 2018, **47**, 2280–2297.
91 Z. Q. Meng, Y. Chao, X. F. Zhou, C. Liang, J. J. Liu, R. Zhang, L. Cheng, K. Yang, W. Pan, M. F. Zhu and Z. Liu, *ACS Nano*, 2018, **12**, 9412–9422.
92 J. Wen, K. Yang, X. C. Ding, H. J. Li, Y. Q. Xu, F. Y. Liu and S. G. Sun, *Inorg. Chem.*, 2019, **58**, 2987–2996.
93 Q. Y. He, Y. Liu, C. L. Tan, W. Zhai, G. H. Nam and H. Zhang, *ACS Nano*, 2019, **13**, 12294–12300.
94 G. Kresse, J. Furthmuller and J. Hafner, *Phys. Rev. B: Condens. Matter Mater. Phys.*, 1994, **50**, 13181–13185.
95 R. Borghese, M. Brucale, G. Fortunato, M. Lanzi, A. Mezzi, F. Valle, M. Cavallini and D. Zannoni, *J. Hazard. Mater.*, 2017, **324**, 31–38.
96 X. Y. Ji, N. Kong, J. Q. Wang, W. L. Li, Y. L. Xiao, S. T. Gan, Y. Zhang, Y. J. Li, X. R. Song, Q. Q. Xiong, S. J. Shi, Z. J. Li, W. Tao, H. Zhang, L. Mei and J. J. Shi, *Adv. Mater.*, 2018, **30**, 11.
97 W. Pan, C. Liu, Y. Li, Y. Yang, W. Li, C. Feng and L. Li, *Bioact. Mater.*, 2022, **13**, 96–104.
98 C. Dai, H. Lin, G. Xu, Z. Liu, R. Wu and Y. Chen, *Chem. Mater.*, 2017, **29**, 8637–8652.
99 B. Xia, B. Wang, J. S. Shi, Y. Zhang, Q. Zhang, Z. Y. Chen and J. C. Li, *Acta Biomater.*, 2017, **51**, 197–208.

100 J. Li, L. Xie, W. Sang, W. Li, G. Wang, H. Tian, Z. Zhang, J. Liu, Q. Fan and Y. Dai, *ChemPhysMater*, 2022, **1**, 51–55.
101 W. C. Huang, C. Y. Xing, Y. Z. Wang, Z. J. Li, L. M. Wu, D. T. Ma, X. Y. Dai, Y. J. Xiang, J. Q. Li, D. Y. Fan and H. Zhang, *Nanoscale*, 2018, **10**, 2404–2412.
102 Z. H. Wang, L. L. Wang, J. R. Huang, H. Wang, L. Pan and X. W. Wei, *J. Mater. Chem.*, 2010, **20**, 2457–2463.
103 J. Wang, Y. Y. Li, L. Deng, N. N. Wei, Y. K. Weng, S. Dong, D. P. Qi, J. Qiu, X. D. Chen and T. Wu, *Adv. Mater.*, 2017, **29**, 6.
104 Q. W. Tian, M. H. Tang, Y. G. Sun, R. J. Zou, Z. G. Chen, M. F. Zhu, S. P. Yang, J. L. Wang, J. H. Wang and J. Q. Hu, *Adv. Mater.*, 2011, **23**, 3542–3547.
105 X. D. Yang, Y. B. Yang, L. N. Fu, M. C. Zou, Z. H. Li, A. Y. Cao and Q. Yuan, *Adv. Funct. Mater.*, 2018, **28**, 9.
106 D. X. Xu, Z. D. Li, L. S. Li and J. Wang, *Adv. Funct. Mater.*, 2020, **30**, 21.
107 Y. Wang, W. Feng, M. Chang, J. Yang, Y. Guo, L. Ding, L. Yu, H. Huang, Y. Chen and J. Shi, *Adv. Funct. Mater.*, 2021, **31**, 2005093.
108 C.-W. Lo, D. Zhu and H. Jiang, *Soft Matter*, 2011, **7**, 5604–5609.
109 Z. L. Zhu, X. L. Cai, S. H. Yi, J. L. Chen, Y. W. Dai, C. Y. Niu, Z. X. Guo, M. H. Xie, F. Liu, J. H. Cho, Y. Jia and Z. Y. Zhang, *Phys. Rev. Lett.*, 2017, **119**, 5.
110 L. D. Xian, A. P. Paz, E. Bianco, P. M. Ajayan and A. Rubio, *2D Mater.*, 2017, **4**, 7.
111 W. Huang, Y. Y. Huang, Y. Y. You, T. Q. Nie and T. F. Chen, *Adv. Funct. Mater.*, 2017, **27**, 15.
112 L. Q. Duan, T. Liu and T. F. Chen, *Biomater. Sci.*, 2021, **9**, 1767–1778.
113 N. Yu, J. N. Li, Z. J. Wang, S. Y. Yang, Z. X. Liu, Y. S. Wang, M. F. Zhu, D. B. Wang and Z. G. Chen, *Adv. Healthcare Mater.*, 2018, **7**, 12.
114 L. F. Wang, Y. Li, L. Zhao, Z. J. Qi, J. Y. Gou, S. Zhang and J. Z. Zhang, *Nanoscale*, 2020, **12**, 19516–19535.
115 K. Plaetzer, B. Krammer, J. Berlanda, F. Berr and T. Kiesslich, *Lasers Med. Sci.*, 2009, **24**, 259–268.
116 A. Gazzi, L. Fusco, A. Khan, D. Bedognetti, B. Zavan, F. Vitale, A. Yilmazer and L. G. Delogu, *Front. Bioeng. Biotechnol.*, 2019, **7**, 15.
117 Y. Ma, Y. X. Ma, M. Q. Gao, Z. H. Han, W. Jiang, Y. Q. Gu and Y. Liu, *Adv. Sci.*, 2021, **8**, 10.
118 X. Li, S. Lee and J. Yoon, *Chem. Soc. Rev.*, 2018, **47**, 1174–1188.
119 F. Q. Fan, L. Wang, F. Li, Y. Fu and H. P. Xu, *ACS Appl. Mater. Interfaces*, 2016, **8**, 17004–17010.
120 L. T. Xu, K. Zhou, H. L. Ma, A. Q. Lv, D. D. Pei, G. P. Li, Y. F. Zhang, Z. F. An, A. Li and G. He, *ACS Appl. Mater. Interfaces*, 2020, **12**, 18385–18394.
121 Z. M. Guo, Y. Liu, X. Cheng, D. Wang, S. B. Guo, M. L. Jia, K. Ma, C. H. Cui, L. Wang and H. Zhou, *Acta Biomater.*, 2020, **110**, 208–220.
122 M. Guo, H. J. Mao, Y. L. Li, A. J. Zhu, H. He, H. Yang, Y. Y. Wang, X. Tian, C. C. Ge, Q. L. Peng, X. Y. Wang, X. L. Yang, X. Y. Chen, G. Liu and H. B. Chen, *Biomaterials*, 2014, **35**, 4656–4666.
123 M. Qiu, D. Wang, H. Huang, T. Yin, W. L. Bao, B. Zhang, Z. J. Xie, N. Xie, Z. Z. Wu, C. C. Ge, Q. Wang, M. Gu, H. L. Kutscher, L. P. Liu, S. Y. Bao, P. N. Prasad and H. Zhang, *Adv. Mater.*, 2021, **33**, 2012562.
124 M. Qiu, Y. Duo, W. Liang, Y. Yang, B. Zhang, Z. Xie, X. Yang, G. Wang, N. Xie, G. Nie, O. A. Alhartomy, A. A. ALGhamdi, S. Wageh, Y. Cao and H. Zhang, *Adv. Funct. Mater.*, 2021, **31**, 17.
125 Y. F. Li, W. Lv, L. Wang, Y. M. Zhang, L. P. Yang, T. Y. Wang, L. Y. Zhu, Y. F. Wang and W. P. Wang, *Nano Res.*, 2021, **14**, 2630–2636.
126 C. Alvarez-Lorenzo, L. Bromberg and A. Concheiro, *Photochem. Photobiol.*, 2009, **85**, 848–860.
127 J. Y. Kim, W. I. Choi, M. Kim and G. Tae, *J. Controlled Release*, 2013, **171**, 113–121.
128 W. Shao, C. Yang, F. Li, J. Wu, N. Wang, Q. Ding, J. Gao and D. Ling, *Nano-Micro Lett.*, 2020, **12**, 147.
129 B. Tian, C. Wang, S. Zhang, L. Feng and Z. Liu, *ACS Nano*, 2011, **5**, 7000–7009.
130 J. C. Ge, M. H. Lan, B. J. Zhou, W. M. Liu, L. Guo, H. Wang, Q. Y. Jia, G. L. Niu, X. Huang, H. Y. Zhou, X. M. Meng, P. F. Wang, C. S. Lee, W. J. Zhang and X. D. Han, *Nat. Commun.*, 2014, **5**, 8.
131 Y. P. Li, T. Y. Lin, Y. Luo, Q. Q. Liu, W. W. Xiao, W. C. Guo, D. Lac, H. Y. Zhang, C. H. Feng, S. Wachsmann-Hogiu, J. H. Walton, S. R. Cherry, D. J. Rowland, D. Kukis, C. X. Pan and K. S. Lam, *Nat. Commun.*, 2014, **5**, 15.
132 C. Mongin, S. Garakyaraghi, N. Razgoniaeva, M. Zamkov and F. N. Castellano, *Science*, 2016, **351**, 369–372.
133 A. M. Merlot, D. S. Kalinowski and D. R. Richardson, *Front. Physiol.*, 2014, **5**, 7.
134 F. Kratz, *J. Controlled Release*, 2008, **132**, 171–183.
135 C. Q. Li, D. H. Zhao, X. L. Hou, B. Zhang, L. B. Song, R. M. Jin, Y. D. Zhao and B. Liu, *Chem. Eng. J.*, 2021, **417**, 10.
136 W. Huang, L. Z. He, J. Ouyang, Q. Chen, C. Liu, W. Tao and T. F. Chen, *Matter*, 2020, **3**, 1725–1753.
137 D. Chimene, D. L. Alge and A. K. Gaharwar, *Adv. Mater.*, 2015, **27**, 7261–7284.
138 Z. X. Tu, G. Guday, M. Adeli and R. Haag, *Adv. Mater.*, 2018, **30**, 27.
139 W. Huang, H. L. Wu, X. L. Li and T. F. Chen, *Chem. – Asian J.*, 2016, **11**, 2301–2311.
140 J. Wang and B. B. Zhang, *Curr. Med. Chem.*, 2018, **25**, 2938–2953.
141 Y. R. Zhou, Y. L. Bai, H. B. Liu, X. H. Jiang, T. Tong, L. R. Fang, D. Wang, Q. Y. Ke, J. G. Liang and S. B. Xiao, *ACS Appl. Mater. Interfaces*, 2018, **10**, 25241–25251.
142 S. H. Tang, M. Chen and N. F. Zheng, *Small*, 2014, **10**, 3139–3144.